Sea ice-associated algae and zooplankton fecal pellets fuel organic particle export in the seasonally ice-covered northwest Labrador Sea

Shao-Min Chen[1], Thibaud Dezutter[2], David Cote[3], Catherine Lalande[2], Evan Edinger[4], Owen A. Sherwood[1]

[1]Department of Earth and Environmental Sciences, Dalhousie University, Halifax, Nova Scotia, Canada

[2]Amundsen Science, Université Laval, Québec City, Québec, Canada

[3]Fisheries and Oceans Canada, Northwest Atlantic Fisheries Centre, St. John's, Newfoundland and Labrador, Canada

[4]Department of Geography and Biology, Memorial University of Newfoundland, St. John's, Newfoundland and Labrador, Canada

Correspondence to: Shao-Min Chen (Shaomin.Chen@dal.ca)

Abstract.

Ocean warming and Arctic sea ice decline are expected to affect biological pump efficiency by altering the timing, quantity, quality, and composition of export production. However, the origins and composition of sinking organic matter are still understudied for the oceans generally, and in ice-covered areas especially. Here we use compound-specific isotope analysis (CSIA) of amino acids (AAs) to investigate the sources and composition of exported organic matter from a sediment trap-derived time-series of sinking particles collected at depths of 469 m and 915 m at the edge of Saglek Bank in the northwest Labrador Sea from October 2017 to July 2019. The outer edge of Saglek Bank is located at the confluence of cold and fresh Arctic outflow and relatively warmer Atlantic waters. The area is subject to seasonal sea ice cover and is a biological hotspot for benthic organisms including deep-sea corals and sponges. Sea ice was present for ~50-60% of the deployment days in both cycles. Phytoplankton blooms at our study site cooccurred with the onset of sea ice melt. Microalgal taxonomy indicated the presence of ice-associated diatoms in the sinking particles during the spring bloom in 2018, confirming that sea ice algae contributed to the organic particle export at our study site. Abundant copepods and copepod nauplii caught in the sediment traps was consistent with a high abundance of copepods in overlying epipelagic waters. Stable carbon isotopes ($\delta^{13}C$) of essential amino acids (EAAs) of the sinking particles revealed a potentially important contribution of sea ice algae as a carbon source at the base of the food web to sinking particles, with only minor modification by microbial resynthesis. Stable nitrogen isotopes ($\delta^{15}N$) of AAs of sinking particles provided independent evidence of the minor bacterial degradation and Bayesian mixing models based on normalized $\delta^{15}N$-AA values revealed dominant contribution of fecal pellets (76-96%) to the sinking particles. Our study demonstrates the importance of sea ice algae and fecal pellets to the biological pump in the seasonally ice-covered northwest Labrador Sea, with sea ice algae exported either directly via passive sinking or indirectly via zooplankton grazing, with fecal pellets dominating the organic particle fluxes.

1 Introduction

The ocean's biological pump sequesters about 10 Pg of carbon per year, which represents up to one-third of anthropogenic carbon emissions to the atmosphere (Sabine et al., 2004; Sabine and Tanhua, 2010). The pump operates by exporting unrespired particulate organic matter (POM) via three pathways: passive sinking ("gravitational pump"), active transport by animals ("migrant pump"), and physical mixing ("mixing pump"; Volk and Hoffert, 1985; Turner, 2015; Nowicki et al., 2022). Despite its importance in global biogeochemical models, the proportional contribution of each biological pump export pathway is poorly estimated. The effects of climate change (i.e., rising temperatures, enhanced ocean stratification and acidification, and changing nutrient availability) compound the uncertainties in biological pump functioning and efficiency (Finkel et al., 2010; Passow and Carlson, 2012; Arrigo and van Dijken, 2015). Arctic and subarctic seas are thought to represent a globally important carbon sink (Bates and Mathis, 2009; MacGilchrist et al., 2014) due to high rates of primary productivity across the expansive continental shelves (Kaltin and Anderson, 2005; Harrison et al., 2013), high nutrient availability (Kaltin et al., 2002, Murata and Takizawa, 2003), and sea-ice and solar dynamics (Rysgaard et al., 2007; Harrison et al., 2013). However, ongoing declines in seasonal sea ice extent and enhanced freshwater input due to global warming has affected particulate organic carbon (POC) export in these regions (Steele et al., 2008; Lalande et al., 2009b; Grebmeier, 2012; Arrigo and van Dijken, 2015). An increase in primary production has been observed in the Arctic (Arrigo and van Dijken, 2015), which could lead to an increase in POC export (Lalande et al., 2009a, b). On the other hand, the loss of sea ice has also been shown to cause a reduction in surface nutrient availability and a shift in plankton community structure from larger celled plankton to picoplankton, which may decrease the POC export to the deep sea (Li et al., 2009; Finkel et al., 2010). The accelerating loss of sea ice necessitates a deeper understanding of factors controlling POC export in ice-covered ecosystems and responses.

In remote regions, sinking particles are typically collected, measured, and characterized using moored sediment traps (Honjo and Doherty, 1988), especially in regions where seasonal sea ice cover constrains remote sensing of ocean colour, preventing the detection of under-ice algal blooms (Strass and Nöthig, 1996; Yager et al., 2001; Fortier et al., 2002; Mundy et al., 2009; Arrigo et al., 2012, 2014). Export flux measurements, phytoplankton and zooplankton identification, and geochemical analyses of sinking particles provide information on 1) sources, cycling, and fate of key elements in the ocean, e.g., carbon and nitrogen, and their biogeochemical roles; and 2) processes and mechanisms that control the fluxes of sinking particles. Nevertheless, it is difficult to identify and quantify the main sources contributing to sinking particles collected in sediment traps. Microalgae and zooplankton taxonomic enumeration can be complicated by large morphological variability within and between species, lack of taxonomic expertise, and inconsistency in identification methods (McQuatters-Gollop et al., 2017). Estimates of biomass or particulate organic carbon (POC) based on composition and abundance data can also be confounded by the wide range in cell sizes within and between functional groups (e.g., diatoms, dinoflagellates, etc; Leblanc et al., 2012). Combining taxonomic methods with biomarker approaches will enhance quantification of the composition of exported sinking particles. This improvement is key to better understanding and predicting the responses of Arctic/subarctic biological pump, marine ecosystems, and benthic communities to a rapidly changing climate.

Stable isotopes of carbon ($\delta^{13}C$) and nitrogen ($\delta^{15}N$) have been widely used to investigate biogeochemical processes in marine ecosystems (Peterson and Fry, 1987; Altabet et al., 1999). Isotopic compositions of sinking organic matter collected in long-term sediment traps record information about sources and cycling of carbon and nitrogen on timescales of months to years (Nakatsuka

et al., 1997; Altabet et al., 1999; Montes et al., 2013). However, traditional measurements of stable isotope values of bulk organic matter can be difficult to interpret due to confounding factors of source variability and heterotrophic modifications (Boecklen et al., 2011). Recent advances in carbon and nitrogen compound-specific isotope analysis (CSIA) of amino acids (AAs) has helped to address these complications (Larsen et al., 2009; Larsen et al., 2013; McMahon et al., 2013; Batista et al., 2014; Ohkouchi et al., 2017; Close, 2019; Shen et al., 2021). Interpretation of δ^{13}C-AA analysis is based on the classification of AAs into essential and non-essential groups. Essential amino acids (EAAs) are synthesized only by autotrophs, and hence their δ^{13}C values remain unchanged with trophic transfers (Larsen et al., 2013; McMahon et al., 2013). Diverse biosynthetic pathways and associated isotopic effects result in distinct and consistent δ^{13}C-EAA signatures of different primary producers, which are reflected in δ^{13}C-EAA patterns of consumers (Hayes, 1993; Larsen et al., 2009). Interpretation of δ^{15}N-AA, on the other hand, is based on different groupings that are independent of those based on δ^{13}C. The δ^{15}N values of source AAs (SrcAAs) undergo little or no δ^{15}N enrichment during trophic transfers while those of trophic AAs (TrAAs) are enriched with increasing trophic position or modified by microbial processing (McClelland & Montoya, 2002). Hence, the complementary but fully independent δ^{13}C-AA and δ^{15}N-AA analyses offer detailed insights about carbon and nitrogen origins, trophic changes, and microbial degradation and allow for more accurate and detailed interpretation of stable isotope data (McMahon et al., 2013; McMahon & McCarthy, 2016).

The goal of this study is to investigate the organic carbon and nitrogen sources and trophic and microbial processing of sinking particles in the seasonally ice-covered northwest Labrador Sea. Two sediment traps were deployed at different depths (469 m and 915 m, respectively) at the outer edge of Saglek Bank from October 2017 to August 2018 and from August 2018 to July 2019. Measurements of particle flux, phytoplankton and zooplankton taxonomy, and bulk stable isotopes were combined with CSIA-AA to characterize the origins, alteration, and transport mechanisms of sinking particles. Together these data help constrain the sources and relative contributions of different components to the sinking particles in the northwest Labrador Sea.

2 Material and methods

2.1 Study site

Located in the north-western section of the Atlantic Ocean, the Labrador Sea is a high-latitude marginal sea of the Atlantic Ocean and an important transition zone connecting Arctic and subarctic ecosystems, bounded by the Labrador and Newfoundland shelves to the west and the southern tip of Greenland to the east (Fragoso et al., 2017). The overall circulation of the Labrador Sea is cyclonic, with layers of distinct water masses in the boundary currents. The upper layer of boundary currents comprises cold and fresh Arctic waters from mixing between the water entering Baffin Bay from eastern Davis Strait, that is cooled in the winter as it circulates within the bay, and the inflow from the Arctic Ocean, that are mainly identified as the Baffin Island Current (BIC) and the Labrador Current (LC; Fig. 1; Tang et al., 2004). Underneath are the relatively warm and saline waters of West Greenland Current (WGC), with a dominant inflow through eastern Davis Strait and a branch deflecting westwards forming a counter-clockwise gyre (Irminger Current) while the remaining waters propagate north (Fig. 1; Yashayaev, 2007; Frajka-Williams et al., 2009). In Baffin Bay, below the WGC water lies the Baffin Bay Deep Water at 1200-1800 m and the Baffin Bay Bottom Water below 1800 m, which have no direct access to the Arctic and Atlantic Oceans due to the relatively shallow sill depths of the Arctic channels and Davis Strait (Tang et al., 2004). The inner shelf of the Labrador Sea is covered by landfast ice with drifting pack ice cover further offshore from January to May each year (Hall et al., 1999; National Snow and Ice Data Center). The study area lies in a transitional zone between the ice-dominated Boreal Polar Province (BPLR) of the Labrador Shelf, and the largely ice-free and deeply convective Atlantic Arctic Province (ARCT) of the Atlantic Polar Biome (Longhurst, 2010), within the path of high iceberg

drifts from the north (Baffin Bay) and the west (Hudson Strait; Marson et al., 2018). Differences in physical-chemical parameters shape variability in phytoplankton community composition and the seasonality of phytoplankton blooms between and within these two provinces (Fratantoni and Pickart, 2007; Yashayaev, 2007; Frajka-Williams and Rhines, 2010; Fragoso et al., 2017). Phytoplankton blooms start on the Labrador shelf from April to early May. These blooms are typically dominated by diatoms, favoured by high silicate concentrations in Arctic waters (Fragoso et al., 2018), and facilitated by vigorous tidal mixing in Hudson Strait (Drinkwater and Harding 2001). From mid-May to June, weaker blooms occur in the central Labrador Sea induced by increased light levels (Frajka-Williams and Rhines, 2010). The strong bottom currents on the Labrador shelf expose hard substrates, providing suitable habitats for deep-sea corals and sponges (Wareham & Edinger, 2007). Observations of abundant and diverse deep-sea corals and sponges are reported at Saglek Bank, forming important habitats for many fish and invertebrate species (Wareham & Edinger, 2007; Dinn et al., 2020). With ongoing global warming and sea ice decline, ice conditions at the study site are projected to be impacted, with up to 70% decrease in winter sea ice extent and a shorter winter ice duration (Han et al., 2019), which may have cascading effects on the phytoplankton community, export fluxes, and in turn, benthic communities.

2.2 Remote sensing

Satellite derived daily-average sea ice concentrations were retrieved at a 12.5 km resolution from the Centre ERS d'Archivage et de Traitement (CERSAT) of the French Research Institute for the Exploration and Exploitation of the Sea (IFREMER) and averaged for a 3° × 3° grid centred at the mooring location (59-62°N, 60-63°W; Fig. 1). Weekly-average chlorophyll *a* (chl *a*) concentrations for the same selected grid (59-62°N, 60-63°W) were derived from Ocean Color (Aqua MODIS, 4 × 4 km; missing data are due to obstacles in observing conditions; https://oceancolor.gsfc.nasa.gov/) and BIO remote sensing group (https://github.com/BIO-RSG). The large areal grid (333 km × 172 km) grid used for sea ice and chl *a* retrieval was necessary to smooth out data coverage gaps.

2.3 Sediment trap and zooplankton net sampling and processing

Two sediment traps were deployed off Saglek Bank on the northwest Labrador slope from October 2017 to August 2018 at a depth of 469 m (bottom depth: 509 m; 60.47°N, 61.26°W; SB-500) and from August 2018 to July 2019 at a depth of 915 m (bottom depth: 1015 m; 60.46°N, 61.16°W; SB-1000) during the annual ArcticNet expeditions of the CCGS *Amundsen* (Table 1; Fig. 1). Both sediment traps (Technicap PPS 3/3; 0.125 m^2 aperture) were equipped with a baffle sieve (diameter: 9.5 mm) covering the trap opening and 24 sampling bottles (265 ml) programmed to rotate every 14 days. Before deployment, each sampling bottle was filled with filtered seawater with a salinity > 36 PSU adjusted using sodium chloride. Sodium borate-buffered formaldehyde (2% v/v) was added to preserve the collected particles during and after deployment. In August 2018 and July 2019, both sediment traps were recovered before the final sampling bottle rotation, therefore the last sampling bottles remained open and were excluded from the study. Zooplankton were sorted from half of the volume of each trap sample under a stereomicroscope and preserved in 4% formalin solution. Zooplankton were counted and identified to the lowest taxonomic level possible (Dezutter et al., 2021). Following the removal of zooplankton, subsamples were analyzed for total particulate matter (TPM), particulate organic carbon (POC) and particulate nitrogen (PN) and converted to daily fluxes (mg m^{-2} d^{-1}) following Dezutter et al. (2021). Microalgal cells were enumerated and counted to the lowest taxonomic level possible using an inverted microscope (Wild Herbrugg) in accordance with Lund et al. (1958). For each sample, a minimum of 100 cells were enumerated along three transects (Genin et al., 2021) at a magnification of 20x for the 2017-2018 deployment and of 60x for the 2018-2019 deployment. Microalgal counts were converted to daily fluxes (cells m^{-2} d^{-1}). For bulk and amino acid stable isotope analyses, samples were washed with Milli-Q water, freeze-dried, and homogenized prior to further analyses.

Zooplankton was opportunistically sampled with a multi-net plankton sampler (Hydrobios, mesh size 200 µm) close to the HiBio-C mooring site (60.47°N, -61.16°E) on July 25, 2021, during the annual CCGS *Amundsen* expedition. The net was opened at 200 m and pulled up all the way to the surface. Once retrieved, zooplankton from the 200-0 m layer were gently poured into incubation chambers filled with filtered seawater (0.2 µm) to clear their gut content for 6-12 hours (Doherty et al., 2021; Stamieszkin et al., 2021). After incubation, zooplankton were transferred into a labelled plastic bag and immediately frozen and stored at -20 ℃ until further analysis.

In the laboratory, 30 to 50 copepods were subsampled from the zooplankton samples using a binocular microscope (Motic SMZ-168). The subsampled copepods were freeze-dried and homogenized until further analysis. Detritus aggregates (clumps of dark-color materials; Fig. 4b) that were collected along with the zooplankton from the incubation chambers were hand-picked into a Petri dish filled with Milli-Q water under the microscope. The collected detritus aggregates were then filtered onto 0.7-µm GF/F filters (Whatman) and freeze-dried until further analysis.

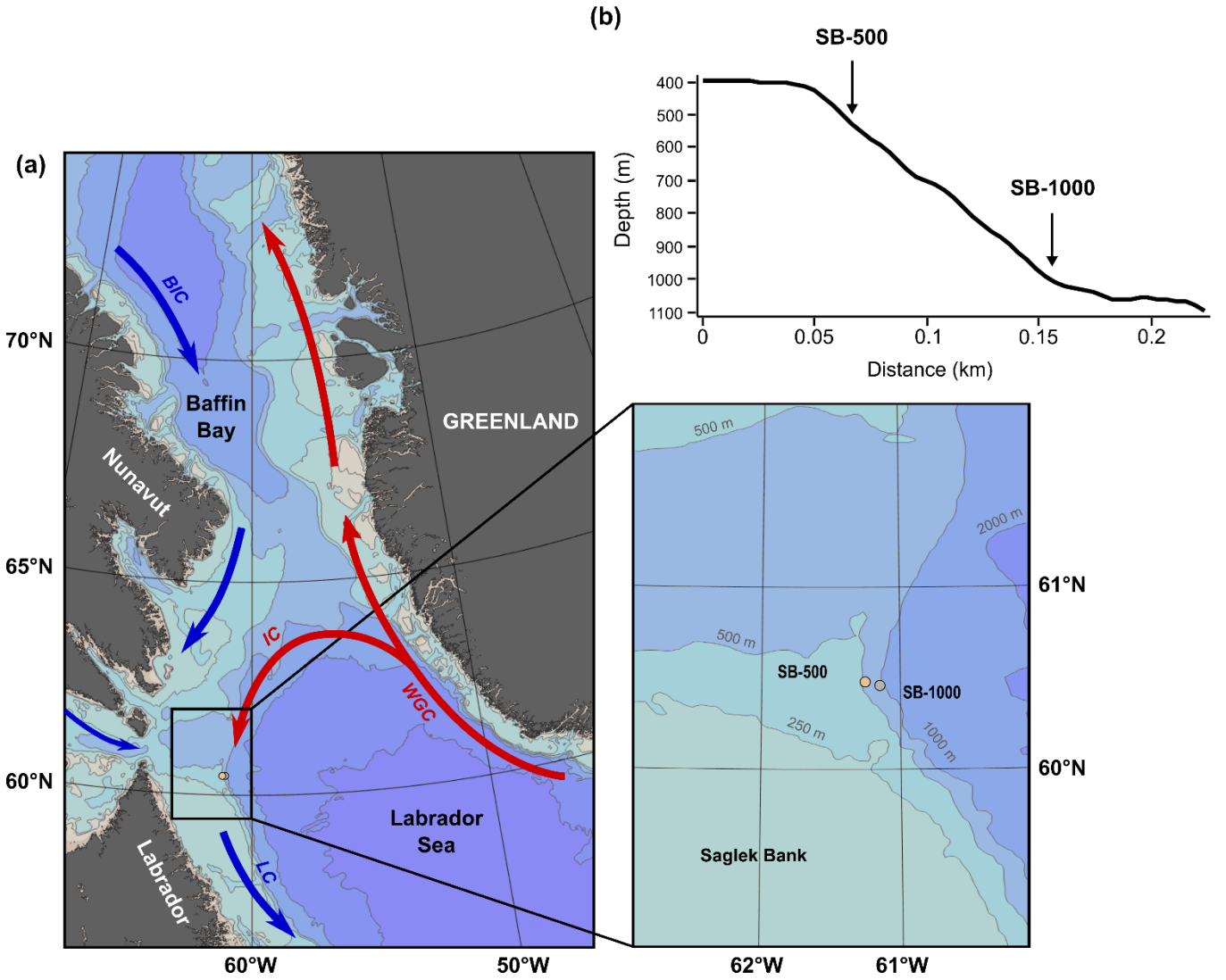

Figure 1 Map and inset detail of study site off Labrador and Nunavut, Canada (a) with bathymetry (grey contours), simplified representation of the main boundary currents (arrows) and sediment trap locations (circles), and (b) cross section of the continent slope where the two sediment traps (SB-500 and SB-1000) were deployed and their depth profiles. Black rectangle represents the area where sea ice concentration and surface chlorophyll *a* concentration were derived for (59-62°N, 60-63°W). Abbreviations: BIC, Baffin Island Current; LC, Labrador Current; IC, Irminger Current; WGC, West Greenland Current. Figure made with Ocean Data View, Schlitzer, 2021.

Table 1 Sediment trap deployment information and sea ice conditions during the deployment in the northwest Labrador Sea.

Trap	Mooring	Latitude (°N)	Longitude (°W)	Trap depth (m)	Deployment date	Recovery date*	Deployment days*	Date of sea ice freeze-up (> 10%)	Date of sea ice melt (<10%)	Deployment days with >10% ice cover (%)	Average areal extent of ice cover during ice-in
SB-500	HiBioA-17	60.47	61.26	469	16-Oct-17	16-Jul-18	274	01-Jan-18	30-Jun-18	62%	44 ± 19%
SB-1000	HiBioC-18	60.46	61.16	915	03-Aug-18	18-Jun-19	319	19-Dec-18	28-May-19	49%	42 ± 14%

***Deployment days for the final sampling bottle rotations were excluded.**

2.4 Bulk and amino acid $\delta^{13}C$ and $\delta^{15}N$ analysis

Subsamples were taken for bulk and amino acid stable isotope analyses (Table S1, S2). Bulk $\delta^{13}C$ and $\delta^{15}N$ were measured in duplicate or triplicate based on the available dry weight of sinking particles. Subsamples for bulk $\delta^{13}C$ analysis were decarbonated in 4% HCl at 80°C for one hour and rinsed in Milli-Q water repeatedly until pH neutralized, following the method of Galy et al. (2007). Decarbonated samples were dried at 50°C overnight. Subsamples for bulk $\delta^{15}N$ analysis were not pre-treated. Bulk $\delta^{13}C$ and $\delta^{15}N$ analysis were carried out at the Canada Excellence Research Chairs Laboratory at Dalhousie University using an Elemental Analyzer (EA; Elementar microcube) coupled with an Isotope Ratio Mass Spectrometer (IRMS; Isoprime 100). Isotopic values were calibrated to co-analyzed reference material and reported in delta notation (δ) in units of per mill "‰" relative to Vienna PeeDee Belemnite (VPDB) and air for $\delta^{13}C$ and $\delta^{15}N$, respectively. Analytical precision based on differences between sample replicates was < 0.15 ‰ for both $\delta^{13}C$ and $\delta^{15}N$.

Approximately 10 mg of organic carbon per sample was required for $\delta^{13}C$-AA and $\delta^{15}N$-AA analyses. Samples with insufficient organic carbon were combined with adjacent samples, if available. Each sample composite included not more than three samples (6 weeks) in total. Combined periods are January 31 to March 3, 2018; April 3 to May 1, 2018; and August 3 to September 18, 2018. Sample composites were hydrolyzed in 6-N HCl (Sigma-Aldrich) at 110 °C for 20 hours, purified and derivatized in batches of 6-7 samples following previously established protocols (Silfer et al. 1991; Larsen et al. 2013; Batista et al. 2014; McMahon et al. 2015; Chen et al. 2022). Samples were derivatized by esterification using isopropanol followed by acylation using trifluoroacetic acid anhydride (Ohkouchi et al., 2017). Each sample batch contained two calibration standards of AA mixtures with known $\delta^{13}C$ and $\delta^{15}N$ values and a lab standard (homogenized Chlorella powder; Organika) processed in the same way as samples. Samples were measured in triplicate for $\delta^{13}C$ and $\delta^{15}N$, bracketed by triplicate injections of calibration standards, using a Trace 1310 Gas Chromatograph (GC) coupled with a Delta V IRMS (Thermo Scientific). A total of twelve AAs were typically resolved: alanine (Ala), glycine (Gly), proline (Pro), valine (Val), leucine (Leu), isoleucine (Ile), asparagine + aspartic acid (Asx), threonine (Thr), serine (Ser), glutamine + glutamic acid (Glx), phenylalanine (Phe), and lysine (Lys). Final $\delta^{13}C$ values were corrected for the isotopic fractionation and the introduction of carbon atoms during derivatization according to Silfer et al. (1991) and normalized against instrument drift between successive triplicate injections of the amino acid standard by applying linear regression (Yarnes and Herszage, 2017). Final $\delta^{15}N$ values were calibrated based on the offset between known and measured values of calibrated standards and normalized against instrument drift by applying linear regression. The average reproducibility of $\delta^{13}C$ was ± 0.3‰ for the internal standard Nle (n = 12), and from ± 0.3‰ (Ala, Leu, Asp, and Phe) to ± 0.8‰ (Lys) for AA standards, respectively (n = 12 for each AA). The average reproducibility of $\delta^{15}N$ was ± 0.4‰ for the internal standard Nle (n = 11), and from ± 0.2‰ (Glu) to ± 0.6‰ (Ala, Val, and Ile) for AA standards, respectively (n = 11 for each AA). The absolute (mol) and relative (mol%) abundances of amino acids were estimated by calibration of mass 44 peak areas against that of internal standard (Nle) using a relative response factor for each AA, following Kaiser and Benner (2005). Yields of total hydrolysable AAs (THAAs) were determined by dividing the total abundance of AAs by the amount of hydrolyzed material.

2.5 Calculations and statistical analyses

To account for the spatio-temporal variations in baseline $\delta^{13}C$ (Larsen et al. 2015; Chen et al. 2022), the $\delta^{13}C$-AA values were internally normalized by subtracting the mean of 5 EAAs (Phe, Leu, Ile, Thr and Val) for each sample (denoted as normalized $\delta^{13}C$). Lys was excluded from the EAA group due to its coelution issues with tyrosine (Tyr). Normalization accounts for influences

from inorganic carbon sources and other environmental parameters, whereas the internal variations between AAs reveal the underlying biochemical mechanisms (Larsen et al., 2015; McMahon et al., 2015; Stahl, 2021; Elliott Smith et al., 2022).

The $\delta^{15}N$ values for THAAs ($\delta^{15}N_{THAA}$) were calculated by summing the mol%-weighted $\delta^{15}N$ values following McCarthy et al. (2013):

$$\delta^{15}N_{THAA} = \sum(\delta^{15}N_i \times mol\%_i) \quad (1)$$

Where $\delta^{15}N_i$ is the calibrated $\delta^{15}N$ value of individual AA and $mol\%_i$ is the mol% of the corresponding AA.

The "metazoan" trophic position (TP_{meta}) of samples was calculated based on calibrated $\delta^{15}N$ values of Glx and Phe, following the equation proposed by Chikaraishi et al. (2009) and modified by Nielsen et al. (2015):

$$TP_{met} = \frac{(\delta^{15}N_{Glx} - \delta^{15}N_{Phe} - 2.9‰)}{6.6‰} + 1 \quad (2)$$

The "protozoan" trophic position (TP_{proto}) was calculated based on calibrated $\delta^{15}N$ values of Ala and Phe, following Décima et al. (2017) and Décima and Landry (2020):

$$TP_{pro} = \frac{(\delta^{15}N_{Ala} - \delta^{15}N_{Phe} - 3.2‰)}{4.5‰} + 1 \quad (3)$$

Three proxies are commonly used to evaluate the degree of heterotrophic bacterial degradation in organic material, based on changes in AA composition or average deviation of $\delta^{15}N$-TrAAs. The percentage of N represented by THAA in total N (THAA-N%) is used as a degradation indicator, where THAA-N% below 38% is considered to indicate diagenetic alteration (Cowie and Hedges, 1992). THAA-N% was calculated, following:

$$THAA - N\% = \frac{\sum(mol_i \times n_i)}{DW \times TN\% \div M_N} \times 100\% \quad (4)$$

Where n is the number of N atoms in individual AA, mol_i is the absolute abundance of this AA, DW is the dry weight of hydrolyzed material, $TN\%$ is the weight percentage of total N, and M_N is the atomic mass of N. Similarly, the percentage of carbon represented by THAA in total organic carbon (THAA-C%) was calculated based on the number of carbon atoms, total organic carbon percentage, and the atomic mass of carbon.

The commonly used degradation index (DI) is based on the changes in the relative concentration of AAs with diagenetic alteration (Dauwe and Middelburg, 1998; Dauwe et al., 1999), and was calculated following Dauwe et al. (1999):

$$DI = \sum_i \left[\frac{var_i - AVG_i}{STD_i}\right] \times fac.coef_i \quad (5)$$

Where var_i is the mol% of each AA in this dataset (Ala, Asp, Glu, Gly, Ile, Leu, Phe, Thr, and Val), and AVG_i and STD_i are the mean and standard deviation of individual AA in the reference dataset from Dauwe et al. (1999), and $fac.coef_i$ is the factor coefficient for the corresponding AA based on the first principal component factor from Table 1 in Dauwe et al. (1999). More positive or negative values of DI indicate relatively fresher or more degraded materials, respectively. Note that DI was calculated without the full suite of AAs used in Dauwe et al. (1999) because these AAs were unable to be resolved across all samples (Ser, Tyr, methionine) or were not measured under the given analytical conditions (histidine, arginine). Calculated DI values are

therefore used for assessing relative changes in diagenetic alteration among samples and may not be directly comparable to literature data. The degree of selective heterotrophic resynthesis was evaluated by calculating the ∑V based on the average deviation of calibrated $\delta^{15}N$ values of TrAAs from their mean, following the formula from McCarthy et al. (2007):

$$\sum V = \frac{1}{n} \sum ABS(\delta^{15}N_i - \delta^{15}N_{mean}) \quad (6)$$

Where n is the number of TrAAs used in the calculation, $\delta^{15}N_i$ are the calibrated $\delta^{15}N$ values of each TrAA (Ile, Leu, Asx, Glx, Pro, and Ala) and $\delta^{15}N_{mean}$ is the average $\delta^{15}N$ of these AAs. Higher ∑V values suggest a higher degree of heterotrophic resynthesis, with values of ~ 1 in fresh phytoplankton biomass, 1 – 2 in fresh zooplankton biomass, and up to ~4 in highly degraded materials such as deep water suspended POM and high molecular weight dissolved organic matter (McCarthy et al., 2007; Yamaguchi et al., 2018; Ianiri et al., 2023).

AA-related indexes were not measured across all 39 individual sediment trap samples because of insufficient organic content or because sample material was exhausted following bulk geochemical analyses. Where possible, temporally adjacent samples were therefore combined to obtain the requisite 10 mg of organic carbon for GC-IRMS analysis. In some samples, one or more AAs were not be resolved due to small peaks or coelution during GC-IRMS runs, also leading to missing values.

Differences in CSIA-AA patterns and parameters were tested between sediment traps, detritus, copepods, and other published end-members using Two Sample T-tests. Prior to carrying out the Two Sample T-test, the residuals of normalized $\delta^{13}C$ and calibrated $\delta^{15}N$ values were tested for univariate normality with Shapiro-Wilks test (R package: stats). To compare the normalized $\delta^{13}C$ signatures between sediment traps and sea ice and pelagic algae, principal component analysis (PCA, R package: FactoMineR) and linear discriminant analysis (LDA, R package: MASS) were performed in R version 4.1.1 with Rstudio interface version 1.4.1717. Standard ellipse areas (SEA) were plotted for each group's bivariate means in the PCA, each enclosing ~40% of the data (Batschelet 1981; Jackson et al., 2011).

Bayesian mixing models based on $\delta^{15}N$-AA were used to estimate the proportional contributions of end-member sources (phytoplankton, zooplankton, fecal pellets, and microbially degraded organic material; Wojtal et al., 2023; Golombek et al., 2023). To ensure robust representation of endmember signatures and because there were no endmember data specific to the Labrador Sea, the data are from all available literature sources (McClelland and Montoya, 2002; Chikaraishi et al., 2009; Hannides et al., 2009, 2013; Yamaguchi and McCarthy, 2018; Doherty et al., 2021). The models were parameterized using endmember means and standard deviations of $\delta^{15}N$-Ala and $\delta^{15}N$-Thr, normalized to $\delta^{15}N$-Phe to account for regional differences in baseline $\delta^{15}N$. These specific AAs have been shown to best separate the potential end-member sources (Doherty et al., 2021). Models were run in R (MixSIAR; Stock and Semmens, 2016) with an uninformative prior and a MCMC chain length of 10^6 (Stock and Semmens, 2016). Model convergence was tested with Geweke and Gelman-Rubin diagnostic tests (Stock and Semmens, 2016). We report the median of results for each end-member to account for skewed distributions of model results.

3 Results

3.1 Environmental Conditions

Sea ice in the study area began forming in early January for both sediment trap deployments and persisted until June in 2018, and May in 2019 (Table 1, Fig. 2a). Sea ice concentration during the ice season averaged around 40% during both deployments (Table 1).

Remotely sensed chl *a* concentration showed peaks in late April 2018 and in early May 2019, when ice concentration was still > 25% (Fig 2a). The timing of these blooms coincided with the onset of > 15 hours of daylight (Astronomical Applications Department of the United States Naval Observatory, "Duration of Daylight"), followed by smaller peaks in chl *a* concentrations (< 2 mg m^{-3}) during the open-water period (defined as sea ice concentration < 10%; Fig. 2a).

Table 2 Total particulate matter (TPM) and particulate organic carbon (POC) daily fluxes, and bulk and amino acid stable isotopes of sinking particles collected from October 2017 to July 2019 in the northwest Labrador Sea.

Trap	Cup	Date opened	Date closed	TPM ($mg\ m^{-2}\ d^{-1}$)	POC ($mg\ C\ m^{-2}\ d^{-1}$)	Bulk $\delta^{13}C$ (‰)	Bulk $\delta^{15}N$ (‰)	TP_{meta}	TP_{proto}	∑V (‰)	DI	THAA yield ($\mu mol\ g^{-1}$)	THAA-C (%)	THAA-N (%)
SB-500	1	16-Oct-17	01-Nov-17	1955	25.5	NA	NA	NA	NA	NA	NA	NA	NA	NA
	2	01-Nov-17	16-Nov-17	959	22.8	NA	NA	NA	NA	NA	NA	NA	NA	NA
	3	16-Nov-17	01-Dec-17	982	19.3	-25.3	6.8	2.1	2.3	2.2	NA	114.9	15.2	50.7
	4	01-Dec-17	16-Dec-17	1116	22.2	-25.3	6.8	2.0	2.3	1.8	-1.1	59.1	10.7	33.6
	5	16-Dec-17	01-Jan-18	591	14.3	-24.7	7.5	NA	NA	NA	NA	NA	NA	NA
	6	01-Jan-18	16-Jan-18	1007	12.9	-24.6	7.0	NA	NA	NA	NA	NA	NA	NA
	7	16-Jan-18	31-Jan-18	603	10.6	-25.0	7.2	NA	NA	NA	NA	NA	NA	NA
	8*	31-Jan-18	15-Feb-18	785	15.1	-25.6	6.3	2.1	2.9	1.8	NA	NA	NA	NA
	9*	15-Feb-18	03-Mar-18	449	10.5	NA	6.7							
	10	03-Mar-18	18-Mar-18	179	5.7	-24.6	7.2	NA	NA	NA	NA	NA	NA	NA
	11	18-Mar-18	03-Apr-18	379	7.8	NA	7.7	2.0	2.4	2.2	-0.9	69.9	NA	36.4
	12*	03-Apr-18	17-Apr-18	294	7.3	-25.4	8.1	2.1	2.6	1.9	-0.8	74.4	12.4	28.1
	13*	17-Apr-18	01-May-18	384	8.5	NA	6.3							
	14	01-May-18	16-May-18	132	4.6	-24.9	6.3	NA	NA	NA	NA	NA	NA	NA
	15	16-May-18	01-Jun-18	285	12.5	-24.3	5.9	2.0	2.0	1.8	-0.4	170.8	18.9	42.4
	16	01-Jun-18	16-Jun-18	86	4.3	-23.8	5.6	NA	NA	NA	NA	NA	NA	NA
	17	16-Jun-18	01-Jul-18	139	5.3	-25.8	6.1	NA	NA	NA	NA	NA	NA	NA
	18	01-Jul-18	16-Jul-18	167	4.4	-24.8	9.3	NA	NA	NA	NA	NA	NA	NA
	Mean ± SD					-24.9 ± 0.6	6.9 ± 0.9	2.0 ± 0.1	2.4 ± 0.1	2.0 ± 0.2	-0.8 ± 0.3	97.8 ± 46.0	14.3 ± 3.6	38.3 ± 8.7
	Annual flux ($g\ m^{-2}\ yr^{-1}$)			214	4.3									
SB-1000	1*	03-Aug-18	19-Aug-18	243	8.4	NA	NA							
	2*	19-Aug-18	03-Sep-18	248	9.3	-25.9	NA	2.3	NA	1.5	0.0	120.0	NA	NA
	3*	03-Sep-18	18-Sep-18	587	16.3	-25.0	8.6							
	4	18-Sep-18	03-Oct-18	1085	23.7	-25.2	6.0	2.1	2.5	2.3	-0.7	78.2	11.5	30.3
	5	03-Oct-18	19-Oct-18	1436	30.4	-25.0	6.7	NA	NA	NA	NA	NA	NA	NA
	6	19-Oct-18	03-Nov-18	719	18.8	-25.4	NA	2.2	2.6	2.2	-0.9	86.0	11.6	NA
	7	03-Nov-18	18-Nov-18	1181	25.2	-25.5	6.7	NA	NA	NA	NA	NA	NA	NA
	8	18-Nov-18	03-Dec-18	798	16.8	-25.1	NA	2.1	2.6	2.1	-0.8	71.0	9.4	NA
	9	03-Dec-18	19-Dec-18	282	9.9	-25.4	7.6	NA	NA	NA	NA	NA	NA	NA
	10	19-Dec-18	03-Jan-19	210	5.2	-26.0	NA	NA	NA	NA	NA	NA	NA	NA
	11	03-Jan-19	19-Jan-19	1029	22.9	-24.6	7.5	2.2	2.9	2.8	-1.3	129.3	17.9	53.1

12	19-Jan-19	02-Feb-19	223	5.9	-26.6	NA	NA	NA	NA	NA	NA	NA	NA
13	02-Feb-19	16-Feb-19	631	11.4	-25.1	6.9	NA	NA	NA	NA	NA	NA	NA
14	16-Feb-19	03-Mar-19	1711	24.5	-24.8	7.1	2.0	2.3	1.9	-1.0	44.6	8.4	24.8
15	03-Mar-19	19-Mar-19	2383	28.4	-24.5	7.8	1.9	2.5	NA	0.5	17.5	1.9	11.7
16	19-Mar-19	03-Apr-19	3017	32.0	-24.8	7.2	2.0	2.7	1.9	2.2	12.4	3.5	9.3
17	03-Apr-19	18-Apr-19	884	13.4	-24.9	NA	2.1	2.8	1.8	-1.1	61.8	11.2	NA
18	18-Apr-19	03-May-19	1360	19.3	-25.0	NA	NA	NA	NA	NA	NA	NA	NA
19	03-May-19	19-May-19	2241	28.4	-24.7	4.5	1.8	2.0	1.6	NA	NA	NA	NA
20	19-May-19	03-Jun-19	2784	35.1	-24.9	5.3	1.9	2.3	1.9	0.0	36.8	7.8	19.9
21	03-Jun-19	18-Jun-19	2036	28.4	-25.2	6.5	NA	NA	NA	NA	NA	NA	NA
Mean ± SD					-25.2 ± 0.5	6.8 ± 1.1	2.0 ± 0.2	2.5 ± 0.3	2.0 ± 0.4	-0.3 ± 1.0	65.8 ± 39.5	9.2 ± 4.7	24.9 ± 15.9
Annual flux (g m^{-2} yr^{-1})			438	7.2									

271 ***CSIA-AA values were combined for adjacent sampling periods (cups).**

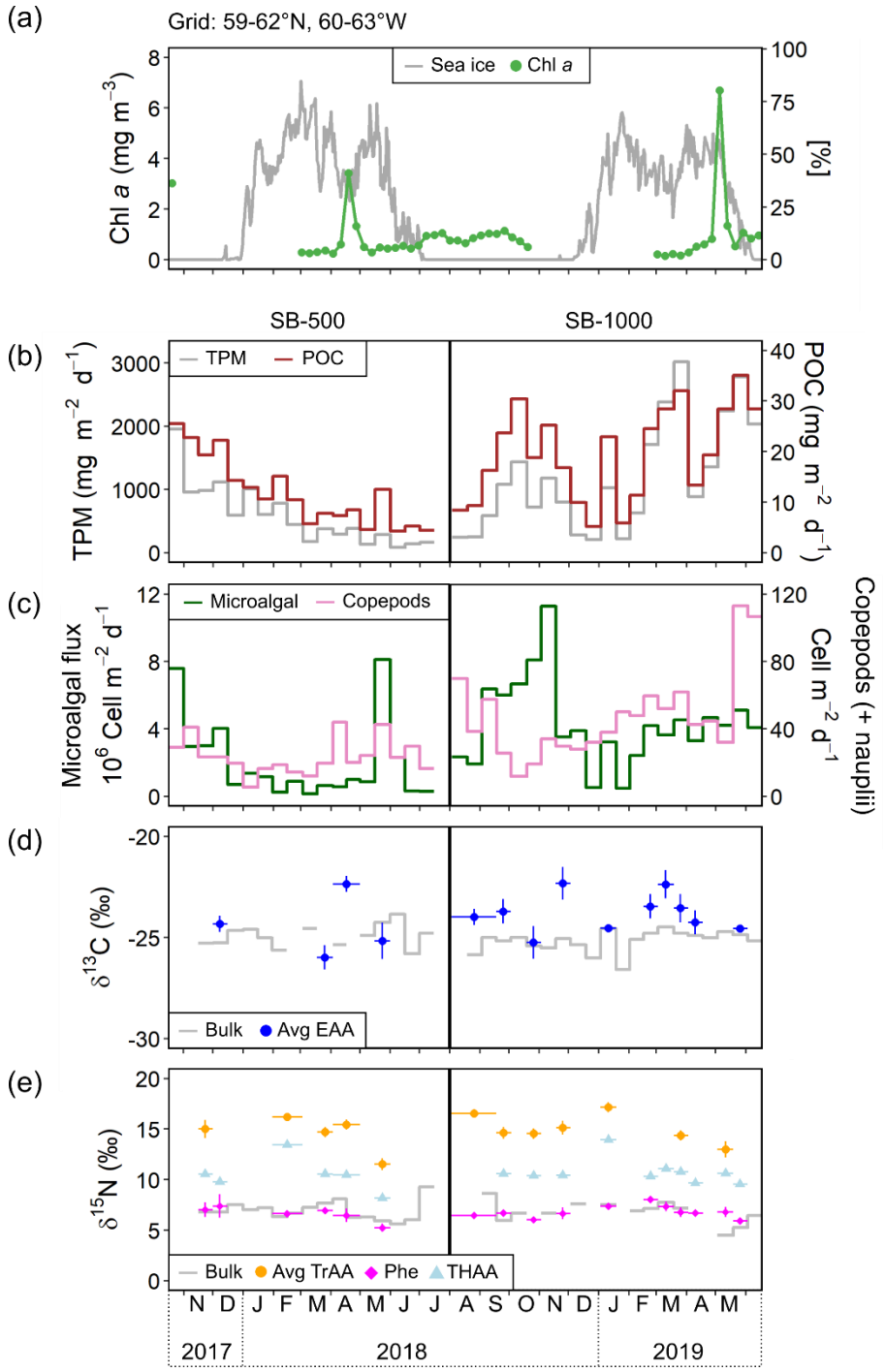

Figure 2 Time-series of (a) satellite derived daily sea ice concentration at a 12.5 km resolution from the Centre ERS d'Archivage et de Traitement (IFREMER) and weekly-averaged chl *a* concentration derived from Ocean Color (Aqua MODIS, 4 × 4 km; missing data are due to obstacles in observing conditions; https://oceancolor.gsfc.nasa.gov/) and BIO remote sensing group (https://github.com/BIO-RSG) for the 3° × 3° grid centred at the mooring site (59-62°N, 60-63°W), (b) total particulate matter (TPM) and particulate organic carbon (POC) fluxes, (c) microalgal flux (diatoms + Chlorophyceae + flagellates) and copepod flux (including copepod nauplii), (d) bulk $\delta^{13}C$ and average $\delta^{13}C$ of five essential amino acids (Avg EAA; Phe, Thr, Ile, Leu, Val), and (e) bulk $\delta^{15}N$, average $\delta^{15}N$ of trophic AAs (Avg TrAA), Phe, and total hydrolysable AAs (THAA) of SB-500 and SB-1000 sinking particles. Vertical error bars show ±1 standard deviation for each sample (n = 3-4). Horizontal error bars show temporal ranges of individual or combined samples (see Sect. 2.4).

3.2 Particulate matter and organic carbon fluxes

Daily fluxes of TPM shared similar trends with POC for each cycle (Fig. 2b). In SB-500, TPM and POC showed an overall decreasing trend from late October 2017 to July 2018, with a small peak in May (Fig. 2b). In SB-1000, TPM and POC peaks were observed in early October and late March and May 2019 (Fig. 2b).

3.3 Microalgal fluxes and swimmers

Diatoms, green algae (Chlorophyceae) and flagellates composed most of the microalgal flux (~97%). Algal fluxes peaked in late October 2017 and late May 2018 at SB-500 and in early November 2018 at SB-1000 (Fig. 2c). Peaks of diatom fluxes were observed in late October, 2017, and from May to June 2018 at SB-500 (Fig. 3a). Centric diatoms contributed the majority of the diatom export in both cycles (Fig. 3b). Shortly before the peak in diatom flux in late May 2018, surface chl *a* maximum was observed in April (Fig. 2a, 3a). During the peak diatom flux in late May 2018, sea ice exclusive species *Nitzschia frigida* and *Melosira arctica* were reported (Fig. 3). Centric and pennate diatom species that are ice-associated, for example, *Fragilariopsis* spp. and *Nitzschia/Pseudo-Nitzschia* spp., were also reported during the peak flux in 2018 (Fig. 3). Relatively high fluxes of green algae (> 2 million cells m^{-2} d^{-1}) were observed in late October and November and in early December 2017 at SB-500 and from early September to early November 2018 at SB-1000 (Fig. 3a). Flagellates dominated the algal fluxes at SB-1000, contributing up to ~75% of the flux (Fig. 3b).

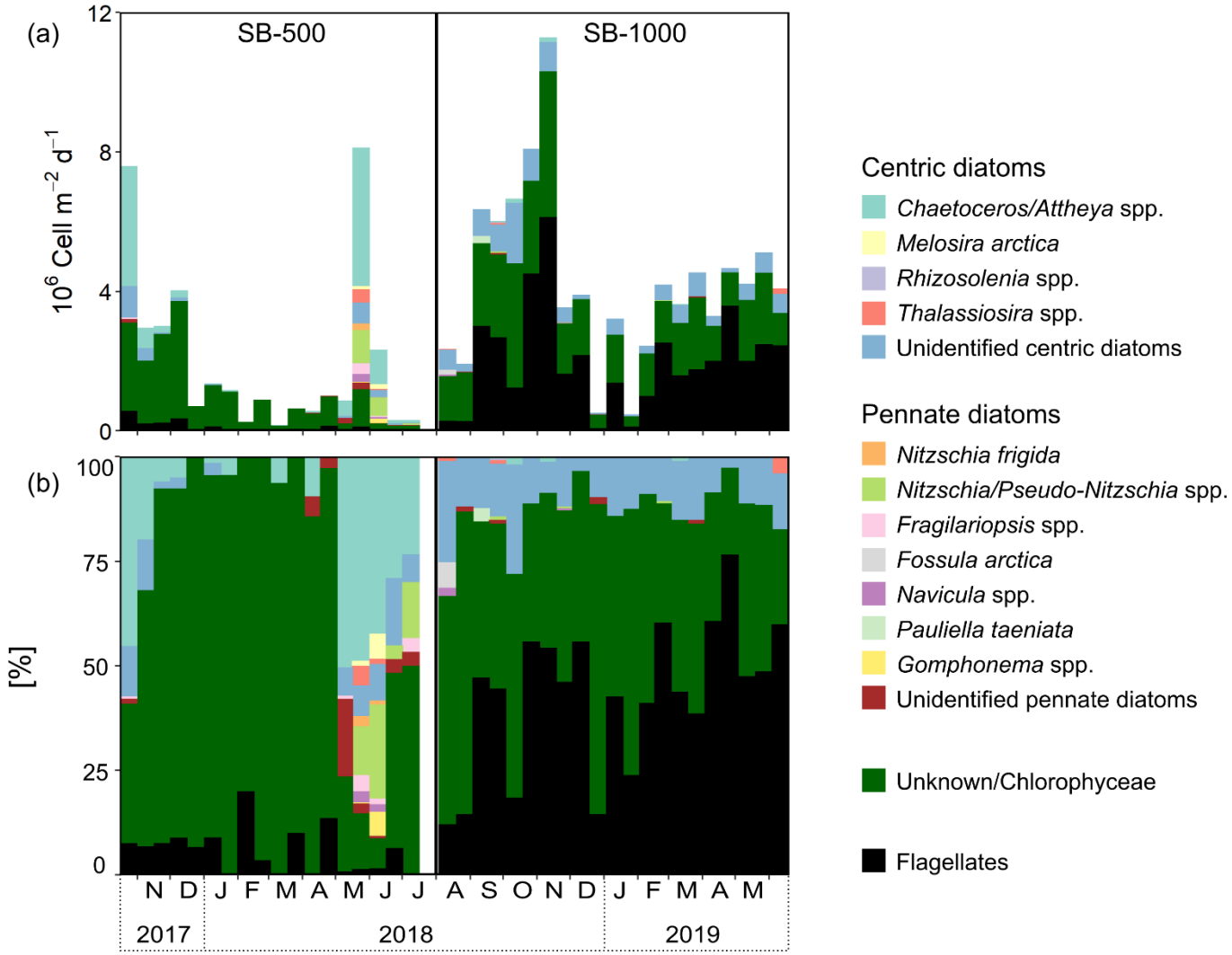

Figure 3 (a) fluxes of diatoms, Chlorophyceae (listed as "unknown" in 2017-2018 cycle), and flagellates and (b) percent contribution of diatoms, Chlorophyceae, and flagellates in sinking particles collected in SB-500 and SB-1000 sediment traps.

Copepods and copepod nauplii dominated the zooplankton community for most of both deployment periods, except when the empty shells of pteropod *Limacina spp.* were dominant in late November 2017 and in September 2018 (data not shown). Peaks of copepod abundances were observed in early November 2017, and early April and late May 2018 at SB-500, and in early August 2018, and late March and late May 2019 at SB-1000 (Fig. 4a). In July 2021, large copepods, e.g., *Calanus* spp., dominated the zooplankton community collected near the sediment trap site (Fig. 4b, c).

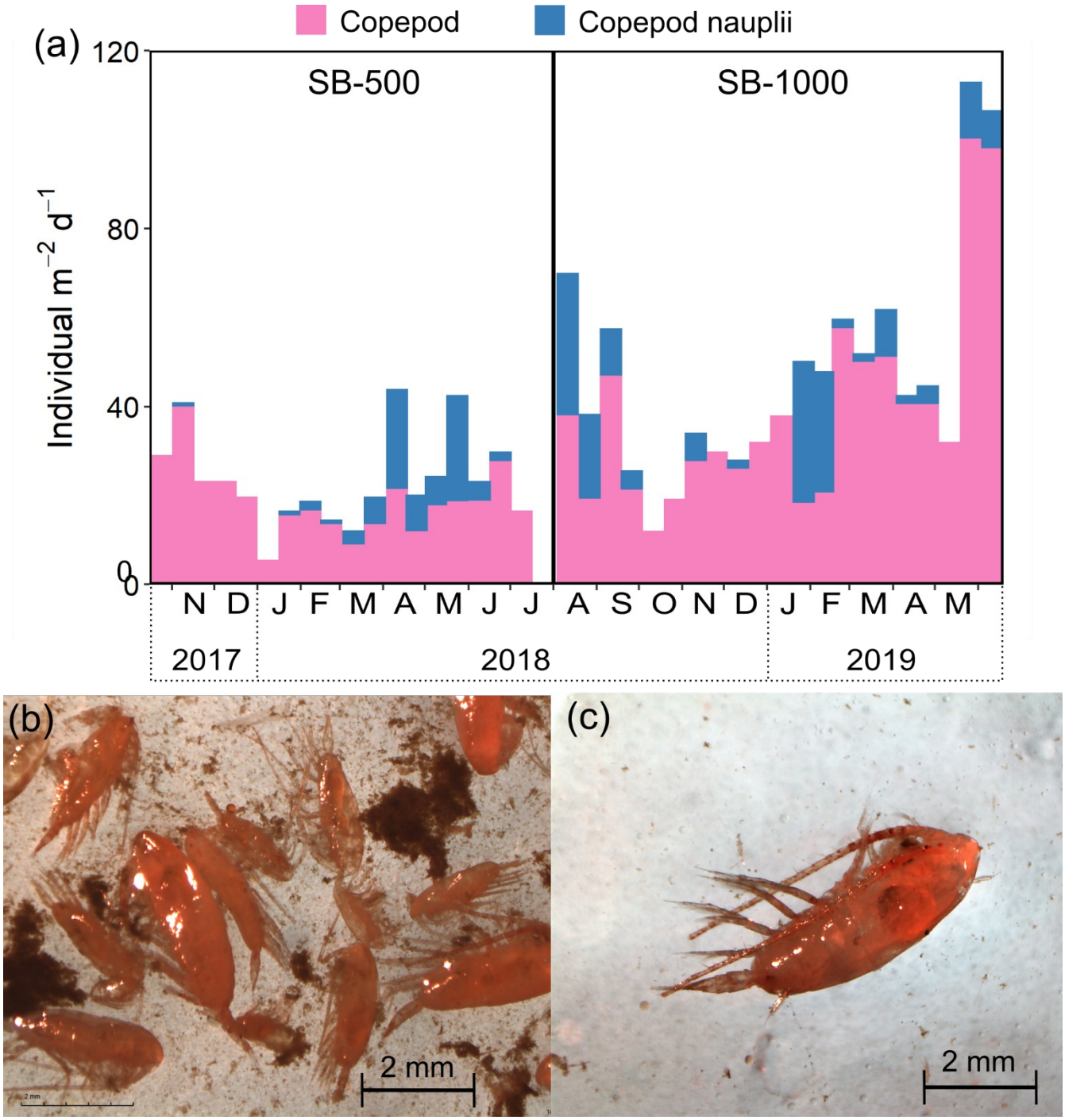

Figure 4 (a) stacked fluxes of copepods and copepod nauplii in sinking particles collected in SB-500 and SB-1000 sediment traps and example images of zooplankton collected in the northwest Labrador Sea in 2021. (b) A mixture of copepods and detritus aggregates in the multi-net samples and (c) example of individual copepod subsampled for CSIA-AA analyses.

3.4 Amino acid compositional variability

THAA yields of the SB-500 and SB-1000 traps averaged 97.8 ± 46.0 and 65.8 ± 39.5 μmol g^{-1}, respectively (Table 2). In SB-500, THAA-C% and THAA-N% averaged 14.3 ± 3.6% and 38.3 ± 8.7%, respectively (Table 2). THAA-C% and THAA-N% of SB-1000 averaged 9.2 ± 4.7% and 24.9 ± 15.9%, respectively (Table 2). DI of the SB-500 and SB-1000 traps averaged -0.8 ± 0.3 and -0.3 ± 1.0, respectively (Table 2). No significant differences were found in THAA yields, THAA-C%, THAA-N% and DI between SB-500 and SB-1000.

3.5 Temporal changes in bulk and amino acid $\delta^{13}C$ and $\delta^{15}N$

Bulk $\delta^{13}C$ values of the SB-500 and SB-1000 traps were similar, varying from -25.8‰ to -23.8‰ and from -26.6‰ to -24.5‰, respectively (Fig. 2d). The average $\delta^{13}C$-EAA values of the sinking particles were more variable than the bulk $\delta^{13}C$ values, fluctuating from -26.0‰ to -22.3‰ with no significant difference (Fig. 2d). Bulk $\delta^{15}N$ values of the SB-500 and SB-1000 traps ranged from 5.6‰ to 9.3‰ and from 4.5‰ to 8.6‰, respectively (Fig. 2e). The $\delta^{15}N$-Phe values, which is commonly used to indicate N source $\delta^{15}N$ value, averaged 6.6 ± 0.7‰ and 6.8 ± 0.6‰ for the SB-500 and SB-1000 traps, respectively, with both minima occurring in May shortly after the surface water chlorophyll peaks (Fig. 2e). The $\delta^{15}N$-TrAA values in both sediment traps averaged ~8.0‰ more elevated than the $\delta^{15}N$-Phe, varying from 11.5‰ to 17.2‰ (Fig. 2e). The $\delta^{15}N$ of total hydrolysable AAs (THAA) averaged 10.5 ± 1.7‰ and 10.7 ± 1.2‰ for the SB-500 and SB-1000 traps, respectively, ranging between $\delta^{15}N$-Phe and $\delta^{15}N$-TrAA (Fig. 2e).

3.6 Amino acid $\delta^{13}C$ and $\delta^{15}N$ patterns

To explore potential carbon sources to export production, we compared the normalized $\delta^{13}C$-AA patterns with algae collected from melted brash ice and pelagic algae collected from deep chlorophyl maximum depth in the northwest Labrador Sea and Baffin Bay in 2019 and 2021 (see details in Chen et al., 2022). Sinking particles obtained during both sampling periods and at both depths shared similar $\delta^{13}C$-EAA patterns, with $\delta^{13}C$ values of ~-4.3‰ for Phe and Val, ~12.5‰ for Thr, ~2.9‰ for Ile and ~-6.8‰ for Leu (Fig. 5a). The $\delta^{13}C$-EAA patterns of sinking particles were more similar to those measured previously for sea ice algae than to those of pelagic algae. Between sinking particles and sea ice algae, only Leu was significantly different (Two-Sample T-Test, $p < 0.05$; Chen et al., 2022) whereas Phe, Thr, and Leu of sinking particles were significantly different from pelagic algae (< 0.05; Fig. 5a; Chen et al., 2022).

Patterns of calibrated $\delta^{15}N$-AA (Fig. 5b) were broadly similar to those for sinking particles reported in other geographical locations, with more enriched $\delta^{15}N$-TrAA and more depleted $\delta^{15}N$-Thr compared to $\delta^{15}N$-SrcAA (Monterey Bay, Shen et al., 2021; Gulf of Maine, Golombek et al., 2024). No significant differences were found in $\delta^{15}N$-AA values between SB-500 and SB-1000 particles (Two Sample T-test, $p > 0.05$). The $\delta^{15}N$ values of individual TrAAs fluctuated from ~12.0‰ to ~17.0‰ (Fig. 5b). The $\delta^{15}N$ values of TrAAs and Thr for sinking particles showed significant distinctions from sea ice and pelagic algae ($p < 0.05$) and detritus ($p < 0.05$ except Val). No significant differences were observed in $\delta^{15}N$-TrAAs between sediment traps and copepods (except Ala). The $\delta^{15}N$-Phe of sinking particles was comparable with sea ice algae ($p > 0.05$) but significantly higher than pelagic algae, copepods, and detritus ($p < 0.05$; Fig. 5b).

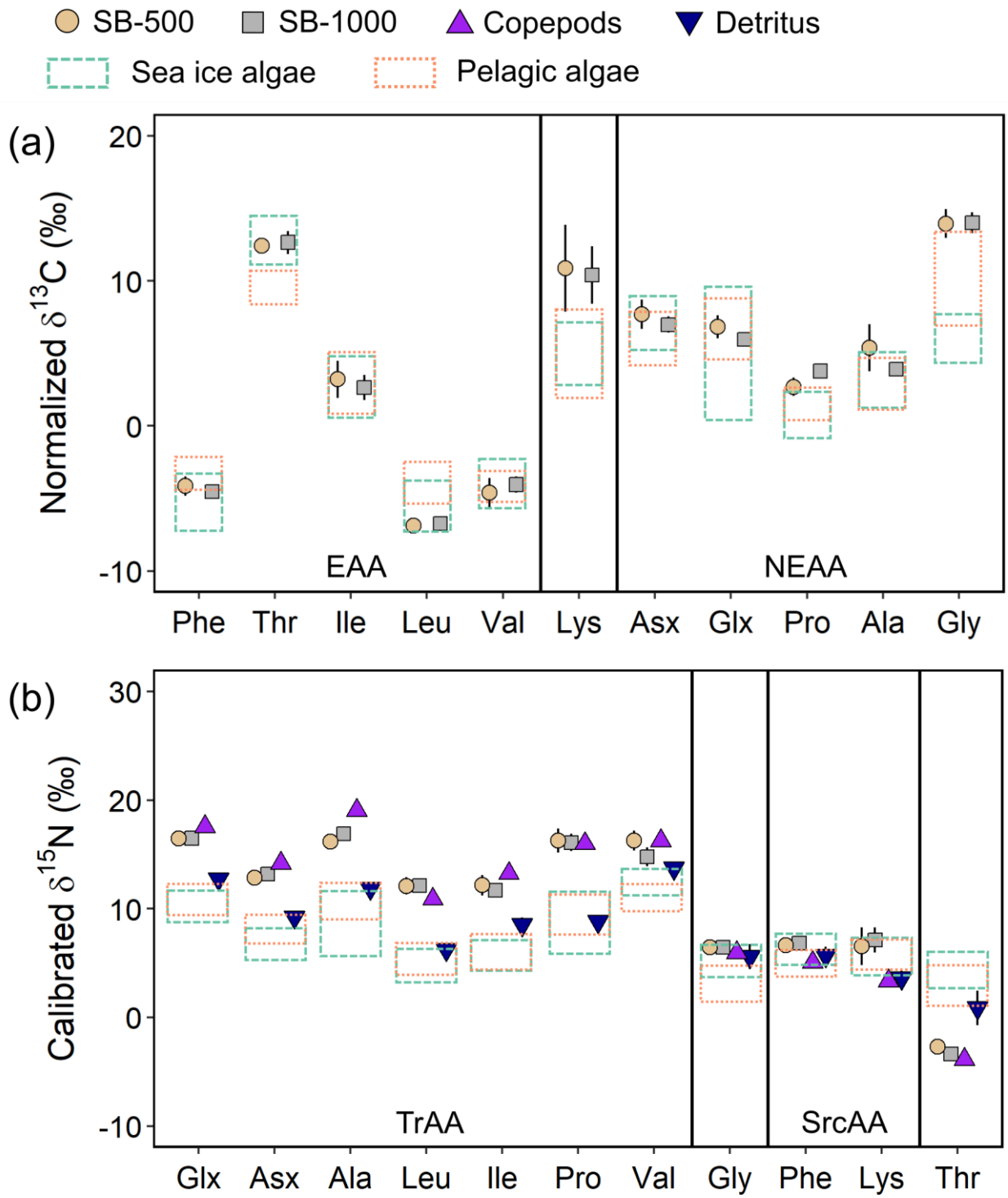

Figure 5 Normalized δ^{13}C-AA patterns (a) and calibrated δ^{15}N-AA patterns (b) of SB-500and SB-1000 sinking particles, copepods and detritus collected close to the mooring site. Data are compared with normalized δ^{13}C-AA and calibrated δ^{15}N-AA patterns of > 3 µm and 0.2-3 µm sea ice and pelagic algae collected from the northwest Labrador Sea and Baffin Bay, respectively (Chen et al., 2022; dashed and dotted rectangles; range: mean ±1 stdev). Error bars show ±1 standard error for each group (SB-500: n = 4-6; SB-1000: n = 7-11; Copepods: n = 3; Detritus = 3). EAA, essential amino acid; NEAA, non-essential amino acid; TrAA, trophic amino acid; SrcAA, source amino acid. Due to coelution with Tyr, Lys was excluded from the EAA group in subsequent analyses.

3.7 Source contributions to sinking particles

To evaluate the potential contributions of sea ice and pelagic algae and heterotrophic bacteria to the sinking particle fluxes, normalized δ^{13}C-AA patterns were compared using PCA (Fig. 6a). PCA based on normalized δ^{13}C-EAA explained 66.3% of the

total variation, with the first two principal components (PC1 and PC2) accounting for 49.9% and 21.4%, respectively (Fig. 6a). The standard ellipses of sinking particles mostly overlapped with each other as well as sea ice algae while clustered apart from pelagic algae and heterotrophic bacteria (Fig. 6a). Linear discriminant analysis (LDA) was then used to classify the sinking particles using the sea ice and pelagic algae and heterotrophic bacteria as the training dataset. Using this approach, 9 out of the 14 measured sinking particle samples were classified as sea ice algae with 87-100% probability (Fig. 6b, Table S5). Three samples were classified as pelagic algae (probability: 62-83%) and two were classified as heterotrophic bacteria (75-98%; Table S5).

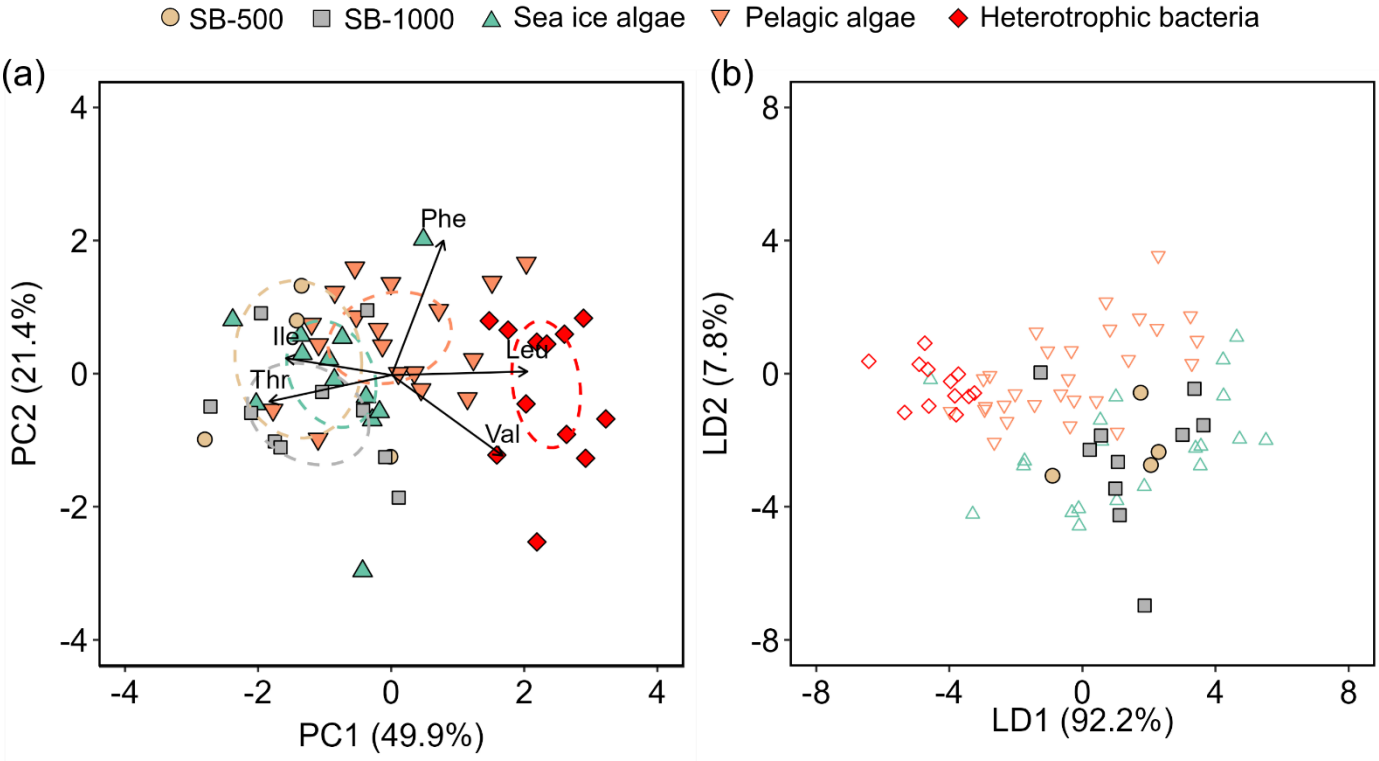

Figure 6 (a) Principal component analysis based on normalized $\delta^{13}C$ values of five essential amino acids showing sinking particles collected in SB-500 and SB-1000 sediment traps in relation to sea ice and pelagic algae from Chen et al. (2022) and heterotrophic bacteria from Larsen et al. (2013). The coloured ellipses represent standard ellipse areas for each corresponding group, containing ~40% of the data. (b) Linear discriminant analysis with the model trained by sea ice and pelagic algae and heterotrophic bacteria data in (a) to predict the classes of sinking particles in SB-500 and SB-1000. Values in parentheses of the axis titles are the percentage variation explained by each axis.

The "metazoan" trophic position (TP_{meta}) values of both sediment traps averaged 2.0 (Fig. 7a). The "protozoan" trophic position (TP_{proto}) averaged 2.4 and 2.6 for the SB-500 and SB-1000 traps, respectively, significantly different from but ranging between detritus (1.7 ± 0.3) and copepods (3.4 ± 0.3; Two Sample T-test, $p < 0.01$; Fig. 7b). Values of the $\sum V$ parameter for microbial resynthesis for SB-500 and SB-1000 sediment traps ranged from 1.8 to 2.2‰ and from 1.5 to 2.8‰, respectively, similar to detritus (1.6-1.9‰; Two Sample T-test, $p > 0.1$) and slightly lower than copepods (2.2-2.7‰; $p < 0.05$; Fig. 7c). No significant offsets were found in TP_{meta}, TP_{proto}, and $\sum V$ values between SB-500 and SB-1000 sediment traps ($p > 0.1$).

Phe-normalized $\delta^{15}N$ of Ala and Thr have been shown to improve characterization of potential end-member contributors to sinking particles (Doherty et al., 2021; Chen et al., 2022; Wojtal et al. 2023). The Phe-normalized $\delta^{15}N$-Ala and $\delta^{15}N$-Thr values were similar between SB-500 and SB-1000 sediment traps (Two Sample T-test, $p > 0.1$), ranging around 10.0‰ and -9.5‰, respectively

and overlapping with literature derived values for fecal pellets ($p > 0.1$; Fig. 7d). Measured copepods shared similar δ^{15}N-Ala and δ^{15}N-Thr values with literature zooplankton values ($p > 0.1$). Measured detritus values ranged between literature phytoplankton, fecal pellets, and degraded OM end-members (Fig. 7d).

A three-end-member Bayesian mixing model based on Phe-normalized δ^{15}N of Ala and Thr demonstrated a dominant contribution (76–96%) of fecal pellets to sinking particles in both sediment traps (Fig. 8, Table S6). Degraded OM contributed 1-3% and phytoplankton contributed 2-17% to the sinking particles (Fig. 8, Table S6). Phytoplankton contribution peaked during the spring bloom in 2018 (Fig. 2a, 3a, 8). No significant differences were found in the modelled contributions of phytoplankton, degraded OM, and fecal pellets to the sinking particles between the SB-500 and SB-1000 traps.

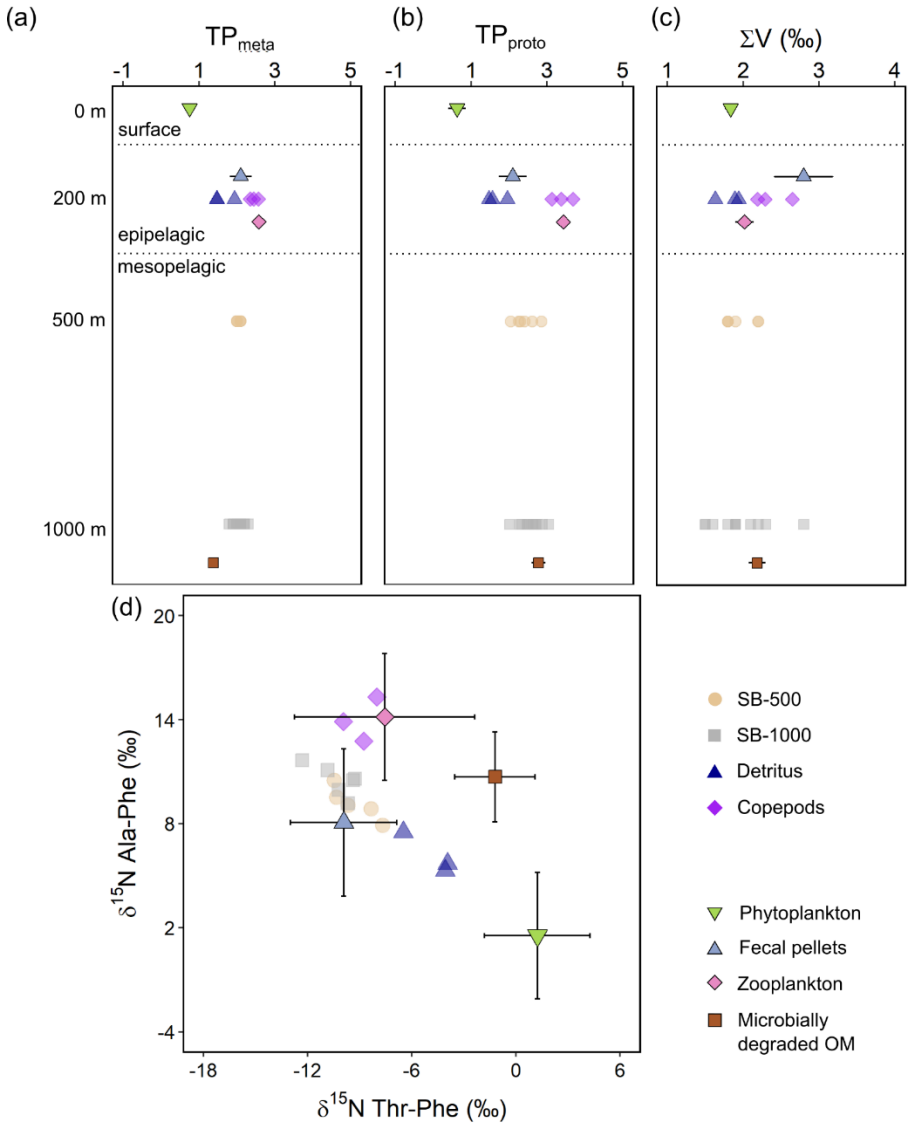

Figure 7 δ^{15}N-AA parameters for trophic positions and microbial resynthesis of sinking particles collected in SB-500 and SB-1000 sediment traps, detritus, and copepods (semi-transparent shapes), compared with means of phytoplankton, fecal pellets, zooplankton, and microbially degraded OM end-members (shapes with error bars). (a) "metazoan" trophic position (TP_{meta}), (b) "protozoan" trophic position (TP_{proto}), and (c) the ∑V parameter in different water layers. (d) Phe-normalized δ^{15}N of Ala and Thr. Error bars show ±1 standard errors for (a)-(c) and standard deviations for (d). End-member distributions are from previously published literature: McClelland and Montoya, 2002; Chikaraishi et al., 2009; Hannides et al., 2009, 2013; Yamaguchi and McCarthy, 2018; Doherty et al., 2021.

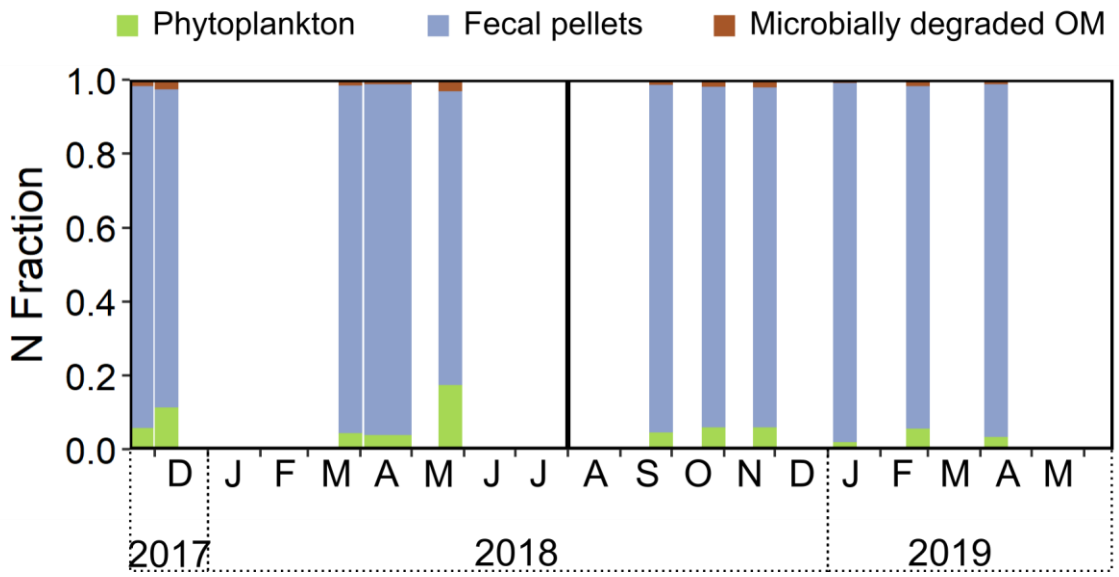

Figure 8 MixSIAR-derived relative contributions of different end-members in sinking particles. The relative N contributions from phytoplankton, fecal pellets, and degraded OM were estimated based on Phe-normalized $\delta^{15}N$ of Ala and Thr. End-member source data are from previously published literature: McClelland and Montoya, 2002; Chikaraishi et al., 2009; Hannides et al., 2009, 2013; Yamaguchi and McCarthy, 2018; Doherty et al., 2021.

4 Discussion

The benthic habitats of Saglek Bank area, including the Labrador Shelf slope, are known to support abundant deep-sea corals and sponges, for example, the gorgonian *Primnoa resedaeformis* and the large sponge *Geodia* spp. (Wareham and Edinger, 2007; Dinn et al., 2020). These deep-water sessile organisms rely on deposition of POM from the surface (Sherwood et al., 2005; Sherwood and Edinger, 2009; Dinn et al., 2020). Therefore, an enhanced understanding of the organic carbon and nitrogen sources and trophic and microbial processing in the sinking particles at the Saglek Bank area is critical. In our study, $\delta^{13}C$-EAA results revealed dominance of relatively "fresh" organic matter (i.e., less microbially degraded) and a potentially high baseline contribution of sea ice algae to sinking particles. The $\delta^{15}N$-AA data suggested sinking particles were dominated by fecal pellets. Despite the more limited temporal resolution of the CSIA-AA data owing to sample size limitations, the combined results suggested that sea ice algae and exported zooplankton fecal pellets can be a critical source of POC and PN for the benthic fauna year-round.

4.1 Contribution of microalgae

Bulk $\delta^{13}C$ values of sinking particles at the study site (-26.6 to -23.8‰) fell toward the lower end of the typical range of marine particulate organic matter from Arctic/subarctic regions (-19 to -26‰; Schubert and Calvert, 2001; Søreide et al., 2006; Belt et al., 2008). The temporal variability of bulk $\delta^{13}C$ was relatively small (~2.0‰) and was not correlated to the more variable $\delta^{13}C$-EAA (~4.0‰; $r^2 = 0.004$; Fig. 2d). Given the relatively low THAA-C% (< 20%), the bulk $\delta^{13}C$ signal in the sinking particles was likely driven by other (non-EAA) carbon-containing compounds (i.e., NEAAs, amino sugars, carbohydrates, lipids, molecularly uncharacterizable organic compounds) and was therefore largely decoupled from $\delta^{13}C$-EAA due to biogeochemical and/or metabolic processing during sinking.

In a previous study, $\delta^{13}C$-EAA in sinking particles collected in sediment traps deployed at 1,200 m depth in Monterey Bay was shown to quantitatively track the bulk $\delta^{13}C$ of surface primary production (Shen et al., 2021). If this principle applies to sinking particles generally, then the $\delta^{13}C$-EAA measured in the Saglek Bank traps would imply that the bulk $\delta^{13}C$ of surface water primary

production ranges from -26.0 to -22.3‰ over an annual cycle. These values bracket a recently modelled estimate of mean annual baseline $\delta^{13}C$ (-23.5‰) at 60°N/60°W in the Labrador Sea but exceed the modelled annual variability by about 3 ‰ (Espinasse et al. 2022). Given the negligible microbial influence on $\delta^{13}C$-EAA values (discussed below), the $\delta^{13}C$-EAA results imply a potentially wider variability in primary producer $\delta^{13}C$ than currently captured in isoscape models of baseline $\delta^{13}C$.

Beyond tracking the $\delta^{13}C$ of primary production, $\delta^{13}C$-EAA signatures are potentially even more useful for quantifying the relative contributions of different primary producer functional groups in marine food webs (Lehman, 2009; Larsen et al., 2013; Schiff et al., 2014; Vokhshoori et al., 2014). Sinking particles collected during both cycles demonstrated similar $\delta^{13}C$-EAA patterns with sea ice and pelagic algae collected from northwest Labrador Sea and Baffin Bay (Chen et al., 2022; Fig. 5), suggesting that exported organic carbon primarily originated from surface primary production, assuming that sea ice and pelagic algae are the major autotrophic sources (Irwin, 1990; Gosselin et al., 1997). Sea ice algae are generally acknowledged to play an important role in primary and export production in the Arctic Ocean, especially in higher latitudes of the Arctic (Hsiao, 1980; Michel et al., 1996; Gosselin et al., 1997; Fernández-Méndez et al, 2014; Fadeev et al., 2021). In our study, a higher similarity was observed between sinking particles and sea ice algae (Two Sample T-test, $p > 0.1$ except Leu), compared to pelagic algae ($p < 0.05$ for Phe, Thr, and Leu; Fig. 5a). This resemblance was further evidenced by the overlap of sinking particles with sea ice algae in the PCA (Fig. 6b), suggesting the carbon in EAAs of the sinking particles may originate largely from sea ice algae.

The large contribution of sea ice algae to the sinking particles is operated via two pathways: direct sinking of ice algal biomass and indirect transfers via heterotrophic processing (e.g., zooplankton grazing). Sea ice algal biomass is generally composed of relatively large cells (> 5 μm; 50-100%) in the Arctic (Gosselin et al., 1997) and hence is exported more efficiently to depth, compared to pelagic algae. Sea-ice or under-ice diatoms typically form large aggregates; when detached from ice, the strands sink rapidly, sporadically contributing large amounts of C to the benthic ecosystem (Fernández-Méndez et al, 2014). Fast-sinking ice-associated diatom aggregates contribute to higher export efficiency and enhanced pelagic-benthic coupling, whereas smaller and slow-sinking flagellate-dominated aggregates are largely recycled in the epipelagic waters (Fadeev et al., 2021). At our study site, sea ice was present for ~50-60% of the deployment days in both cycles (Table 1). Both chl *a* maxima in early April, 2018 and early May, 2019 coincided with sea ice breakups (defined as sea ice concentration < 50% for more than five consecutive days), suggesting a potential release of sea ice algae to the water column by the ice melt (Fig. 2a; Michel et al., 1993). Following the chl *a* maxima, the persistent phytoplankton blooms with a smaller magnitude (< 2 mg m^{-3}) during the open-water period could be governed by nutrient limitation (Fig. 2a; Leu et al., 2015). In the Labrador Sea, light is the primary limiting factor to primary production for most of the year, which is largely governed by daylight periods, sea ice cover, and snow depth, controlling the timing and initiation of under-ice blooms (Mundy et al., 2009, 2014; Leu et al., 2015), whereas nutrients becomes co-limiting or limiting in summer/autumn as they become depleted within the mixed layer, especially for nitrate on the Labrador Shelf (Harrison and Li, 2007). Nevertheless, remote-sensing of ocean color only accounted for phytoplankton blooms in open water and thus under-ice algal growth remained "invisible" and its magnitude was uncertain.

Direct sinking of sea ice algae was also evident by the microalgal taxonomy of our sinking particles. Sea ice and pelagic algae are often dominated by centric and pennate diatoms with species reported in both habitat types (Hsiao, 1980; Melnikov, 1998; Poulin et al., 2011), for example, *Fragilariopsis* spp. and *Nitzschia/Pseudo-Nitzschia* spp, which were also observed in our samples (Fig. 3). Microalgal counts revealed a dominance of *Chaetoceros/Attheya* spp. in the fall diatom fluxes in 2017 and the fluxes in 2018 while unidentified centric diatoms dominated the fall fluxes in 2018 and the spring fluxes in 2019 (Fig. 3b). Although it is difficult to tell what fraction of the observed diatoms were originated from sea ice or pelagic habitats, the observation of sea ice exclusive

species *N. frigida* and *M. arctica* in the sinking particles of the northwest Labrador Sea confirmed the cooccurrence of sea ice algae in exported carbon (Fig. 3; Lalande et al., 2019a). The occurrence of *Nitzschia frigida* and *Melosira arctica* cooccurred with the dominance of *Chaetoceros/Attheya* spp. in May 2018, shortly after the surface chl *a* maximum in April associated with the ice melt, suggesting concurrent pelagic production and sea ice algal release induced by sea ice breakup in 2018 (Fig. 2a, 3). Although the direct export of *Nitzschia frigida* and *Melosira arctica* accounted for only a small fraction, the magnitude of sea ice algal export remains unknown, given the fact that many diatom species can be either from sea ice or pelagic habitats (Fig. 3b). Further, taxonomic analysis provides a visual representation of plankton cells exported through passive sinking but does not account for other organic matter components, such as fecal pellets and detritus. Therefore, the taxonomic counts only represent a portion of exported sea ice algae whereas δ^{13}C-EAA can trace the other portion that cannot be visually identified (e.g., degraded, assimilated, or excreted).

In terms of indirect carbon export from surface primary producers, flux of fecal pellets from zooplankton grazing is an important but highly variable component, which is governed by variation in sea ice/pelagic algae and zooplankton biomass and community composition (Turner, 2015). Sea ice algae were found to have higher nutritional quality compared to phytoplankton with an elevated essential fatty acid content and thereby may be a better food source for consumers (Park et al., 2002; Arrigo and Thomas, 2004; McMahon et al., 2006; Amiraux et al., 2021). The importance of sea ice algae as food supply for zooplankton grazers has been reported in Hudson Bay (Runge and Ingram, 1988), Frobisher Bay (Grainger and Hsiao, 1990), Canadian Arctic Archipelago (Michel et al., 1996), Barents Sea (Scott et al., 1999, 2001), and northern Baffin Bay (Michel et al., 2002). A more recent biomolecular study also revealed active feeding on sea ice algae by copepods *Calanus glacialis* under seasonal sea ice long before ice melt and the development of ice-edge blooms in the Northern Bering Sea (Durbin and Casas, 2014). Overall, δ^{13}C-EAA signatures revealed a dominance of relatively "fresh" organic matter (i.e., less microbially degraded) and a potentially high baseline contribution of sea ice algae in sinking particles (via direct or indirect export), which was consistent with previous observations that sea ice algae could be either exported via fast-sinking aggregates (e.g., in Beaufort Sea, Carey, 1987; in Eurasian Basin, Fernández-Méndez et al, 2014), or ingested by zooplankton and exported as fecal materials (e.g., in Canadian Arctic Archipelago, Michel et al., 1996). The contribution of fecal pellets to our sinking particles was further evidenced by the presence of intact fecal pellets and the independent δ^{15}N-AA analyses, discussed in the section below.

4.2 Organic nitrogen composition of sinking particles

The δ^{15}N-THAA values represent the mass-balanced N isotopic signature of all AAs and were 2-7‰ more elevated than bulk signals (Fig. 2e), indicating that other N-containing organic compounds (inorganic clays, nucleic acids, pigments, amino sugars, and uncharacterizable OM; Hedges et al., 2001; Kienast et al. 2005; Batista, 2016; McMahon and McCarthy, 2016), must be isotopically lighter than THAA. These offsets further reinforce the idea that bulk and compound-specific isotope signatures may be decoupled from each other, particularly in detrital materials such as sinking POM (Batista et al. 2014; Golombek et al. 2024).

In addition to microbial degradation (discussed separately in section 4.3 below), variations in δ^{15}N-AA reflect mainly baseline δ^{15}N values of source N and heterotrophic transfers (Ohkouchi et al., 2017). The δ^{15}N-Phe in sinking particles (6.7 ± 0.6‰) was within range of the δ^{15}N of nitricline nitrate (Sherwood et al. 2021) and sea ice algae (Fig. 7b) in the study region. This indicates that δ^{15}N-Phe in the sinking particles preserves baseline δ^{15}N variability. The δ^{15}N of TrAAs, on the other hand, were substantially higher than that of ice or pelagic algae, indicating isotopic enrichment by heterotrophic metabolisms. Based on calculated values of TP_{meta} (2.0 ± 0.2), metazoan heterotrophy increased the trophic position of sinking particles, over that of fresh phytoplankton, by one unit. The slightly higher values of TP_{proto} (2.5 ± 0.3), indicated an additional 0.5 unit increase in trophic position resulting

from protozoan heterotrophy. These results indicate that AAs in sinking POM were not sourced *directly* from algal detritus, but rather cycled through metazoan and protozoan metabolisms.

The distribution of sinking particles in Phe-normalized δ^{15}N-Ala vs δ^{15}N-Thr space helped resolve the relative contribution of end-member source materials (phytoplankton, zooplankton, fecal pellets, and microbial degraded OM), to the sinking particles (Fig. 7d). The theoretical basis for the separation of endmember data by δ^{15}N-Ala and δ^{15}N-Thr was outlined in Doherty et al. (2021). Briefly, Thr exhibits 'reverse' fractionation (becomes more negative) with metazoan metabolism (McMahon and McCarthy, 2016) and effectively distinguishes animal metabolism (zooplankton and fecal pellets) from microbial metabolism (phytoplankton and microbially degraded OM). Alanine, on the other hand, has a higher sensitivity than the canonical TrAA Glu to protozoan heterotrophy (Gutiérrez-Rodríguez et al., 2014; Décima et al., 2017), and therefore increases the separation between zooplankton and phytoplankton, particularly if mesozooplankton feed on protozoan microzooplankton (Doherty et al., 2021). Fecal pellets plot between zooplankton and phytoplankton along the δ^{15}N-Ala axis, presumably because they comprise a mixture of zooplankton biomass, gut microbiota and undigested phytoplankton (Doherty et al, 2021). Normalization of δ^{15}N-Ala and δ^{15}N-Thr to δ^{15}N-Phe accounts for regional differences in baseline δ^{15}N, allowing comparison of measured to literature data. As a demonstration of validity of this approach, the measured copepods plot within the uncertainty envelope of literature zooplankton (Fig. 7d). Similarly, the previously published sea ice and pelagic algae collected in the study region overlap with literature phytoplankton values (Chen et al., 2022).

Bayesian mixing modeling based on Phe-normalized δ^{15}N of Ala and Thr quantified contributions of source end-members to sinking particles. The zooplankton end-member was not included in the mixing model for the sinking particles because zooplankton individuals were sorted and removed from the sediment trap samples (See Sect. 2.3). Assuming phytoplankton, fecal pellets, and microbially degraded OM are the major N sources to the AA pool in sinking particles, the MixSIAR mixing model suggested a dominant contribution of fecal pellets throughout the two years (76-96%; Fig. 8). The contribution of fecal pellets was evidenced by the observation of intact fecal pellet fluxes to the sinking particles in the 2018-2019 cycle (Fig. S2; note that fecal pellets were not counted for the 2017-2018 cycle). This was consistent with the observations of sustained copepod communities in removed swimmers from sediment traps (Fig. 4a) and highly abundant large-bodied copepods caught in the plankton sampler at the study site (Fig. 4b, c) as well as previous observations of copepod dominance in subarctic Labrador Sea (Darnis et al., 2022). During phytoplankton blooms, the contribution of direct phytoplankton export was up to 17% (Fig. 8). Note that fecal pellets used in our mixing model consist of data collected from salp, amphipod, krill and mixed community samples that involve herbivory, carnivory, and detritivory feeding (Doherty et al., 2021) and thus may lead to a large uncertainty of the end-member; a future more refined copepod fecal pellet end-member may help improve the accuracy of the model estimation. As a further demonstration of model validity, we also applied a four end-member mixing model which included zooplankton on our measured copepod and detritus (Table S7). Copepod samples were accurately classified within the "zooplankton" end-member (56-87%), while detritus samples were classified as "phytoplankton" (31-55%) and "fecal pellets" (33-54%). Since the detritus aggregates were collected along with the zooplankton from the plankton net (see Sect. 2.3), they were likely contributed by large particles (marine snow) that originate from aggregated phytoplankton (phytodetritus) and fecal matter (Turner, 2015).

4.3 Preservation of AA-specific isotope signals

Sediment traps may be influenced by lateral transport or resuspension of aged sediment which is more degraded (Rea and Hovan, 1995; Hwang et al., 2010). The sediment traps were deployed at the outer edge of Saglek Bank (Fig. 1), exposed to strong bottom

currents and vertical mixing from the Hudson Strait outflow (Fig. 1; Hecker et al., 1980; Harding, 1998; Drinkwater and Harding, 2001; Wareham & Edinger, 2007; Ostiguy, 2022; de Froe et al., 2024). Inputs of these degraded materials have the potential to alter and confound either of the δ^{13}C-EAA or δ^{15}N-AA source attribution approaches described above. However, the influence of resuspended sediments is considered minor, at least to the AA pool, based on multiple lines of evidence. First, the established diagenetic indicator THAA-N% in the sinking particles averaged 38.3 ± 8.7% in SB-500 and 24.9 ± 15.9% in SB-1000 (Table 2), which (at times) exceeded the generally accepted lower limit (38%) for living biomass (Cowie and Hedges, 1992). Second, the range of δ^{15}N-Phe values argues against any impact of microbial metabolisms (i.e., extracellular hydrolysis; Hannides et al., 2009; Yamaguchi et al., 2017) that would otherwise increase δ^{15}N-Phe above the regional δ^{15}N baseline of ~6-7 ‰ (Sherwood et al. 2021). Third, while the ΣV parameter for total microbial resynthesis appeared to have low diagnostic utility in distinguishing among potential OM sources, the average ΣV across both traps (2.0 ± 0.4) was within range of fresh zooplankton and fecal pellet biomass (Fig. 7c). Finally, both AA-specific isotopic source attribution approaches explicitly account for bacterial carbon inputs in the case of δ^{13}C-EAA (Fig. 6) and microbial resynthesis in the case of δ^{15}N-AA (Fig. 7d and Fig. 8). These two fully independent approaches indicate minimal microbial degradation or alteration of source specific isotope signatures in the sinking particles throughout both sediment trap deployments, despite significant temporal variations in TPM and POC fluxes. Overall, it appears that AA-specific isotope signatures are well preserved in the sediment traps, despite and independently of the apparent effects of seasonal and depth related resuspension on bulk geochemistry.

4.4 Exported fecal pellets

The fecal-pellet-like δ^{15}N-AA signatures in our sinking particles and Bayesian mixing model outputs revealed a potential dominance of fecal pellets to exported POM at the study site (Fig. 7d). Sinking fecal pellets serve as an important source of organic material for benthic communities but are hard to quantify (Pilskaln and Honjo, 1987; Wilson et al., 2013). The collection of recognizable fecal pellets and its proportion in sinking particles largely vary with depth, season, location and is affected by zooplankton diets and other enhancing/inhibiting mechanisms during sedimentation (Noji, 1991; Hargrave et al., 1994; Wilson et al., 2013). During sedimentation, fecal pellets are likely to be modified and repackaged several times and become unrecognizable as fecal pellets, making it difficult for visual identification (Noji, 1991). For example, an earlier study estimated a low fecal pellet contribution to POC in a sediment trap collected under permanent ice cover in the Arctic (< 20%), which was derived from enumeration of two types of pellets (cylindrical and ellipsoid; Hargrave et al., 1994). Nevertheless, our results agreed with more recent studies that discovered substantial contribution of fecal pellets from large copepods to vertical export (up to > 60% of the POC flux) in other polar regions; e.g., Fram Strait (Lalande et al., 2011), northern Baffin Bay (Sampei et al., 2004), Beaufort Sea (Juul-Pedersen et al., 2010), and the Southern Ocean (Dagg et al., 2003; Gleiber et al., 2012; Décima et al., 2023). Recent applications of Bayesian mixing model using Phe-normalized δ^{15}N of Ala and Thr revealed an increasing contribution of fecal pellets to both small and large particles with increasing depth in North Pacific, indicating fecal pellet production by zooplankton and disaggregation into smaller particles at mesopelagic depths (> 50% in the mid mesopelagic; Doherty, 2021; Wojtal et al. 2023). A recent model study suggested that sinking fecal pellets accounted for 50-90% of total carbon export for most low-latitude seas (Nowicki et al., 2022). Physical transport of suspended POC by vertical mixing, seasonal mixed layer detrainment, eddy subduction, and large-scale ocean circulation also play an important role in exporting POC to depth (Omand et al., 2015; Dall'Olmo et al., 2016; Nowicki et al., 2022). For example, based on mixed-layer depth data from Argo floats and satellite estimates of POC, the largest mixed-layer pump can be found in high latitude regions in the North Atlantic, Southern Ocean, and north-west Pacific,

accounting for on average 23% of estimates of the biological carbon pump (Dall'Olmo et al., 2016). Glider observations complemented by high-resolution modelling revealed that eddy-driven POC flux can contribute up to half of the total POC export during spring blooms in highly productive subpolar oceans, such as North Atlantic (Omand et al., 2015).

Overall, our findings suggested that sea ice algae and zooplankton fecal pellets may fuel export productivity to the mesopelagic zone in a seasonally ice-covered region. This has important ecological implications for global warming and declines in sea ice in the Arctic and subarctic oceans (Pabi et al., 2008). Sea ice declines represent habitat loss and reduced fatty acid quality for sea ice-reliant species (Post et al., 2013). This reduction accompanied by younger and thinner ice, freshening surface water, and less ice-covered area in the Arctic/subarctic, may also induce changes in community structures and phenology of zooplankton, and hence impacting fecal pellet export and food supply to benthic communities (Post et al., 2013; Leu et al., 2015; Turner, 2015). Although primary production and POC fluxes were predicted to increase in polar oceans as a result of longer ice-free periods, other mechanisms may limit the delivery of POM to benthic ecosystems (Sweetman et al., 2017). First, ocean warming accelerates remineralization and microbial degradation in the water column and hence may reduce the effectiveness of POM export to depth (Riebesell et al., 2009; Turner, 2015). Increased stratification caused by surface warming and freshwater input from sea ice melting limits deep-water ventilation and reduces nutrient supply to surface waters. The weakened deep-water intrusion may reduce the strength of mixed layer pump that acts as an important pathway for POM export in high latitude seas (Dall'Olmo et al., 2016). Reduced nutrient supply shifts the surface plankton communities from dominance by diatoms and large zooplankton towards those dominated by picoplankton and small zooplankton, thereby reducing the strength of biological pump and the sedimentation of organic particles to depth (Li et al., 2009; Finkel et al., 2010; Turner, 2015). This may further deprive benthic communities of organic matter supply, which are predicted to impact biodiversity hotspots, such as those inhabited by deep-sea corals and sponges (Levin and Le Bris, 2015; Sweetman et al., 2017). Hence, these habitats are particularly vulnerable to changes in food quality and quantity in the changing Arctic/subarctic oceans.

5 Conclusions

In this study, we applied CSIA-AA proxies on sinking particles time series collected in sediment traps at depths of 469 m and 915 m in the northwest Labrador Sea (~60°N) to explore the sources and composition of organic carbon and nitrogen in sinking organic matter at the Arctic/subarctic boundary. The sinking particles δ^{13}C-EAA patterns indicated that sea ice algae are an important food source to higher trophic levels and that surface primary production was largely preserved in exported organic matter at the study site. Additionally, δ^{15}N-AA results independently verified the minor bacterial contribution to sinking particles and revealed dominant animal sources (fecal pellets and zooplankton) to the sinking flux. Overall, these results have significant implications for the use of CSIA-AA in biogeochemical and ecological studies of marine environments. The use of CSIA-AA in sinking particles time series obtained from moored sediment traps provides quantitative estimates of plankton and fecal pellet contributions to carbon export in the ocean, which may help improve the accuracy of flux estimates derived from counting methods and biogeochemical models. Combined with conventional analyses, such as plankton analyses and flux measurements, CSIA-AA may fulfil the promise of precise and high-resolution delineation of marine sinking organic matter in space and time. Climate-related ocean changes may further limit food availability for deep-water benthic assemblages, such as deep-sea corals and sponges (Levin and Le Bris, 2015; Sweetman et al., 2017). We suggest that future work should expand CSIA-AA measurements on sinking particles collected by sediment trap time series globally and establish multi-proxy data repository for vulnerable ecozones. CSIA-AA end-member data for estimating sinking particle composition should be better constrained, especially for δ^{13}C-EAA. Direct measurements of end-member data from the study region will improve the accuracy of sources estimation. More accurate

quantitative estimates of sinking particle composition and processing are beneficial for future studies to predict the biogeochemical and ecological responses in important deep-sea ecosystems to on-going changing climate.

Data availability

Data are available in the supplementary material (Table S1, S2, S3).

Author contribution

S-MC, DC, EE and OAS contributed to conception and design of the study. S-MC and TD contributed to sampling. TD contributed to flux measurements and microalgal and zooplankton counts. S-MC and OAS contributed to sample processing, CSIA-AA and bulk stable isotope measurements, and data analysis. DC, EE, and CL contributed to data interpretation. S-MC wrote the manuscript with input from all the co-authors.

Competing interests

The authors declare that they have no conflict of interests.

Acknowledgements

Funding for this study was provided by an NSERC Discovery Grant to OAS (RGPIN-2018-05590), NSERC Ship Time grants to OAS (544990-2020) and EE (515528-2018), and DFO funding to the Marine Conservation Targets program. Moorings were collected on board the Canadian research icebreaker *CCGS Amundsen* as part of the ArcticNet Hidden Biodiversity (HiBio) project. Logistical support was provided by the Amundsen Science program, which is supported by the Canada Foundation for Innovation through Université Laval. We would like to express our gratitude for all the officers and crew members of the Canadian Coast Guard Ship *Amundsen* for their professional support with sediment trap and zooplankton sampling. We also thank Shawn Meredyk from Amundsen Science for leading mooring deployments and recoveries, Maxime Geoffroy, Eugenie Jacobsen, and Jordan Sutton for helping with zooplankton sampling, Claire Normandeau for bulk stable isotope analyses, Karen Stamieszkin for valuable discussion about zooplankton analyses, and Alexandre Normandeau for providing the depth profiles.

References

Altabet, M.A., Pilskaln, C., Thunell, R., Pride, C., Sigman, D., Chavez, F. and Francois, R.: The nitrogen isotope biogeochemistry of sinking particles from the margin of the Eastern North Pacific. Deep Sea Research Part I: Oceanographic Research Papers, 46(4), 655-679, 1999.

Amiraux, R., Archambault, P., Moriceau, B., Lemire, M., Babin, M., Memery, L., Massé, G. and Tremblay, J.E.: Efficiency of sympagic-benthic coupling revealed by analyses of n-3 fatty acids, IP25 and other highly branched isoprenoids in two filter-feeding Arctic benthic molluscs: Mya icrozoo and Serripes groenlandicus. Organic Geochemistry, 151, 104160, https://doi.org/10.1016/j.orggeochem.2020.104160, 2021.

Arrigo, K.R. and Thomas, D.N.: Large scale importance of sea ice biology in the Southern Ocean. Antarctic Science, 16(4), 471-486, 2004.

Arrigo, K.R., Perovich, D.K., Pickart, R.S., Brown, Z.W., Van Dijken, G.L., Lowry, K.E., Mills, M.M., Palmer, M.A., Balch, W.M., Bahr, F. and Bates, N.R.: Massive phytoplankton blooms under Arctic sea ice. Science, 336(6087), 1408-1408, 2012.

Arrigo, K.R., Perovich, D.K., Pickart, R.S., Brown, Z.W., Van Dijken, G.L., Lowry, K.E., Mills, M.M., Palmer, M.A., Balch, W.M., Bates, N.R. and Benitez-Nelson, C.R.: Phytoplankton blooms beneath the sea ice in the Chukchi Sea. Deep Sea Research Part II: Topical Studies in Oceanography, 105, 1-16, 2014.

Arrigo, K.R. and van Dijken, G.L.: Continued increases in Arctic Ocean primary production. Progress in Oceanography, 136, 60-70, https://doi.org/10.1016/j.pocean.2015.05.002, 2015.

Astronomical Applications Department of the United States Naval Observatory (no date) Duration of Daylight/Darkness Table for One Year. Available at: https://aa.usno.navy.mil/data/Dur_OneYear (Accessed: 06 November 2023).

Bates, N.R. and Mathis, J.T.: The Arctic Ocean marine carbon cycle: evaluation of air-sea CO 2 exchanges, ocean acidification impacts and potential feedbacks. Biogeosciences, 6(11), 2433-2459, 2009.

Batista, F. C., Ravelo, A. C., Crusius, J., Casso, M. A., & McCarthy, M. D.: Compound specific amino acid δ15N in marine sediments: A new approach for studies of the marine nitrogen cycle, Geochimica et Cosmochimica Acta, 142, 553-569, 2014.

Batista, F.C.: An examination of the marine nitrogen cycle: insights from novel stable nitrogen isotopic approaches. University of California, Santa Cruz, 2016.

Batschelet, E.: Circular Statistics in Biology. Academic Press, London, 1981.

Bélanger, S., Ehn, J.K. and Babin, M.: Impact of sea ice on the retrieval of water-leaving reflectance, chlorophyll a concentration and inherent optical properties from satellite ocean color data. Remote Sensing of Environment, 111(1), 51-68, 2007.

Belt, S.T., Massé, G., Vare, L.L., Rowland, S.J., Poulin, M., Sicre, M.A., Sampei, M. and Fortier, L.: Distinctive 13C isotopic signature distinguishes a novel sea ice biomarker in Arctic sediments and sediment traps. Marine Chemistry, 112(3-4), 158-167, https://doi.org/10.1016/j.marchem.2008.09.002, 2008.

Boecklen, W.J., Yarnes, C.T., Cook, B.A. and James, A.C.: On the use of stable isotopes in trophic ecology. Annual Review of Ecology, Evolution and Systematics, 42(1), 411-440, https://doi.org/10.1146/annurev-ecolsys-102209-144726, 2011.

Buesseler, K.O., Antia, A.N., Chen, M., Fowler, S.W., Gardner, W.D., Gustafsson, O., Harada, K., Michaels, A.F., Rutgers van der Loeff, M., Sarin, M. and Steinberg, D.K., An assessment of the use of sediment traps for estimating upper ocean particle fluxes. Journal of Marine Research, 65(3), 345-416, DOI: 10.1357/002224007781567621, 2007.

Carey Jr, A.G.: Particle flux beneath fast ice in the shallow southwestern Beaufort Sea, Arctic Ocean. Marine Ecology Progress Series, 247-257, 1987.

Chen, S.M., Mudie, P. and Sherwood, O.A.: Amino acid δ13C and δ15N fingerprinting of sea ice and pelagic algae in Canadian Arctic and Subarctic Seas. Frontiers in Marine Science, 1868, https://doi.org/10.3389/fmars.2022.976908, 2022.

Chikaraishi, Y., Ogawa, N.O., Kashiyama, Y., Takano, Y., Suga, H., Tomitani, A., Miyashita, H., Kitazato, H. and Ohkouchi, N.: Determination of aquatic food-web structure based on compound-specific nitrogen isotopic composition of amino acids. Limnology and Oceanography: methods, 7(11), 740-750, https://doi.org/10.4319/lom.2009.7.740, 2009.

Close, H.G.: Compound-specific isotope geochemistry in the ocean. Annual Review of Marine Science, 11, 27-56, https://doi.org/10.1146/annurev-marine-121916-063634, 2019.

Colombo, J.C., Silverberg, N. and Gearing, J.N.: Amino acid biogeochemistry in the Laurentian Trough: vertical fluxes and individual reactivity during early diagenesis. Organic Geochemistry, 29(4), 933-945, 1998.

Cowie, G.L. and Hedges, J.I., Sources and reactivities of amino acids in a coastal marine environment. Limnology and Oceanography, 37(4), 703-724, https://doi.org/10.4319/lo.1992.37.4.0703, 1992.

Dagg, M.J., Urban-Rich, J. and Peterson, J.O.: The potential contribution of fecal pellets from large copepods to the flux of biogenic silica and particulate organic carbon in the Antarctic Polar Front region near 170 W. Deep Sea Research Part II: Topical Studies in Oceanography, 50(3-4), 675-691, https://doi.org/10.1016/S0967-0645(02)00590-8, 2003.

Dall'Olmo, G., Dingle, J., Polimene, L., Brewin, R.J. and Claustre, H.: Substantial energy input to the mesopelagic ecosystem from the seasonal mixed-layer pump. Nature Geoscience, 9(11), 820-823, 2016.Dauwe, B. and Middelburg, J.J.: Amino acids and hexosamines as indicators of organic matter degradation state in North Sea sediments. Limnology and Oceanography, 43(5), 782-798, https://doi.org/10.4319/lo.1998.43.5.0782, 1998.

Darnis, G., Geoffroy, M., Dezutter, T., Aubry, C., Massicotte, P., Brown, T., Babin, M., Cote, D. and Fortier, L.: Zooplankton assemblages along the North American Arctic: Ecological connectivity shaped by ocean circulation and bathymetry from the Chukchi Sea to Labrador Sea. Elementa: Science of the Anthropocene, 10(1), 00053, 2022.

Dauwe, B., Middelburg, J.J., Herman, P.M. and Heip, C.H.: Linking diagenetic alteration of amino acids and bulk organic matter reactivity. Limnology and Oceanography, 44(7), 1809-1814, https://doi.org/10.4319/lo.1999.44.7.1809, 1999.

Décima, M., Landry, M.R., Bradley, C.J. and Fogel, M.L.: Alanine δ15N trophic fractionation in heterotrophic protists. Limnology and Oceanography, 62(5), 2308-2322, https://doi.org/10.1002/lno.10567, 2017.

Décima, M. and Landry, M.R.: Resilience of plankton trophic structure to an eddy-stimulated diatom bloom in the North Pacific Subtropical Gyre. Marine Ecology Progress Series, 643, 33-48, https://doi.org/10.3354/meps13333, 2020.

Décima, M., Stukel, M.R., Nodder, S.D., Gutiérrez-Rodríguez, A., Selph, K.E., Dos Santos, A.L., Safi, K., Kelly, T.B., Deans, F., Morales, S.E. and Baltar, F.: Salp blooms drive strong increases in passive carbon export in the Southern Ocean. Nature Communications, 14(1), 425, https://doi.org/10.1038/s41467-022-35204-6, 2023.

de Froe, E., Yashayaev, I., Mohn, C., Vad, J., Mienis, F., Duineveld, G., Kenchington, E., Head, E., Ross, S.W., Blackbird, S. and Wolff, G.A.: Year-long benthic measurements of environmental conditions indicate high sponge biomass is related to strong bottom currents over the Northern Labrador shelf, 2024.

Dezutter, T., Lalande, C., Darnis, G. and Fortier, L.: Seasonal and interannual variability of the Queen Maud Gulf ecosystem derived from sediment trap measurements, Limnology and Oceanography, 66, S411-S426, https://doi.org/10.1002/lno.11628, 2021.

Dinn, C., Zhang, X., Edinger, E. and Leys, S.P. Sponge communities in the eastern Canadian Arctic: species richness, diversity and density determined using targeted benthic sampling and underwater video analysis, Polar Biology, 43(9), 1287-1305, https://doi.org/10.1007/s00300-020-02709-z, 2020.

Doherty, S.: Stable Isotope Signatures of Zooplankton Fecal Pellets in Particulate Organic Matter (Doctoral dissertation, University of Miami), 2021.

Doherty, S.C., Maas, A.E., Steinberg, D.K., Popp, B.N. and Close, H.G.: Distinguishing zooplankton fecal pellets as a component of the biological pump using compound-specific isotope analysis of amino acids. Limnology and Oceanography, 66(7), 2827-2841, https://doi.org/10.1002/lno.11793, 2021.

Drinkwater, K.F. and Harding, G.C.: Effects of the Hudson Strait outflow on the biology of the Labrador Shelf. Canadian Journal of Fisheries and Aquatic Sciences, 58(1), 171-184, 2001.

Drinkwater, K., Colbourne, E., Loeng, H., Sundby, S. and Kristiansen, T.: Comparison of the atmospheric forcing and oceanographic responses between the Labrador Sea and the Norwegian and Barents seas. Progress in Oceanography, 114, 11-25, https://doi.org/10.1016/j.pocean.2013.03.007, 2013.

Durbin, E.G. and Casas, M.C.: Early reproduction by Calanus glacialis in the Northern Bering Sea: the role of ice algae as revealed by molecular analysis. Journal of Plankton Research, 36(2), 523-541, 2014.

Edwards, M.S., Turner, T.F. and Sharp, Z.D., Short-and long-term effects of fixation and preservation on stable isotope values (δ13C, δ15N, δ34S) of fluid-preserved museum specimens. Copeia, 2002(4), 1106-1112, https://doi.org/10.1643/0045-8511(2002)002[1106:SALTEO]2.0.CO;2, 2002.

Elliott Smith, E.A., Fox, M.D., Fogel, M.L. and Newsome, S.D.: Amino acid δ13C fingerprints of nearshore marine autotrophs are consistent across broad spatiotemporal scales: An intercontinental isotopic dataset and likely biochemical drivers. Functional Ecology, 36(5), 1191-1203, https://doi.org/10.1111/1365-2435.14017, 2022.

Espinasse, B., Sturbois, A., Basedow, S.L., Hélaouët, P., Johns, D.G., Newton, J. and Trueman, C.N.: Temporal dynamics in zooplankton δ13C and δ15N isoscapes for the North Atlantic Ocean: Decadal cycles, seasonality, and implications for predator ecology. Frontiers in Ecology and Evolution, 10, 986082, 2022.

Fadeev, E., Rogge, A., Ramondenc, S., Nöthig, E.M., Wekerle, C., Bienhold, C., Salter, I., Waite, A.M., Hehemann, L., Boetius, A. and Iversen, M.H.: Sea ice presence is linked to higher carbon export and vertical microbial connectivity in the Eurasian Arctic Ocean. Communications Biology, 4(1), 1255, https://doi.org/10.1038/s42003-021-02776-w, 2021.

Fernández-Méndez, M., Wenzhöfer, F., Peeken, I., Sørensen, H.L., Glud, R.N. and Boetius, A.: Composition, buoyancy regulation and fate of ice algal aggregates in the Central Arctic Ocean. PLoS One, 9(9), e107452, 2014.

Finkel, Z.V., Beardall, J., Flynn, K.J., Quigg, A., Rees, T.A.V. and Raven, J.A.: Phytoplankton in a changing world: cell size and elemental stoichiometry. Journal of plankton research, 32(1), 119-137, https://doi.org/10.1093/plankt/fbp098, 2010.

Fortier, M., Fortier, L., Michel, C. and Legendre, L.: Climatic and biological forcing of the vertical flux of biogenic particles under seasonal Arctic sea ice. Marine Ecology Progress Series, 225, 1-16, 2002.

Fragoso, G.M., Poulton, A.J., Yashayaev, I.M., Head, E.J. and Purdie, D.A.: Spring phytoplankton communities of the Labrador Sea (2005–2014): pigment signatures, photophysiology and elemental ratios. Biogeosciences, 14(5), 1235-1259, https://doi.org/10.5194/bg-14-1235-2017, 2017.

Fragoso, G.M., Poulton, A.J., Yashayaev, I.M., Head, E.J., Johnsen, G. and Purdie, D.A.: Diatom biogeography from the Labrador Sea revealed through a trait-based approach. Frontiers in Marine Science, 5, 297, https://doi.org/10.3389/fmars.2018.00297, 2018.

Frajka-Williams, E., Rhines, P.B. and Eriksen, C.C.: Physical controls and mesoscale variability in the Labrador Sea spring phytoplankton bloom observed by Seaglider. Deep Sea Research Part I: Oceanographic Research Papers, 56(12), 2144-2161, https://doi.org/10.1016/j.dsr.2009.07.008, 2009.

Frajka-Williams, E. and Rhines, P.B.: Physical controls and interannual variability of the Labrador Sea spring phytoplankton bloom in distinct regions. Deep Sea Research Part I: Oceanographic Research Papers, 57(4), 541-552, https://doi.org/10.1016/j.dsr.2010.01.003, 2010.

Fry, B.: Food web structure on Georges Bank from stable C, N, and S isotopic compositions. Limnology and Oceanography, 33(5), 1182-1190, https://doi.org/10.4319/lo.1988.33.5.1182, 1988.

Francois, R., Honjo, S., Krishfield, R. and Manganini, S.: Factors controlling the flux of organic carbon to the bathypelagic zone of the ocean. Global Biogeochemical Cycles, 16(4), 34-1, https://doi.org/10.1029/2001GB001722, 2002.

Fratantoni, P.S. and Pickart, R.S.: The western North Atlantic shelfbreak current system in summer. Journal of Physical Oceanography, 37(10), 2509-2533, https://doi.org/10.1175/JPO3123.1, 2007.

Galy, V., Bouchez, J. and France-Lanord, C.: Determination of total organic carbon content and δ13C in carbonate-rich detrital sediments. Geostandards and Geoanalytical Research, 31(3), 199-207, https://doi.org/10.1111/j.1751-908X.2007.00864.x, 2007.

Gaye, B., Fahl, K., Kodina, L.A., Lahajnar, N., Nagel, B., Unger, D. and Gebhardt, A.C.: Particulate matter fluxes in the southern and central Kara Sea compared to sediments: Bulk fluxes, amino acids, stable carbon and nitrogen isotopes, sterols and fatty acids. Continental Shelf Research, 27(20), 2570-2594, https://doi.org/10.1016/j.csr.2007.07.003, 2007.

Genin, F., Lalande, C., Galbraith, P.S., Larouche, P., Ferreyra, G.A. and Gosselin, M.: Annual cycle of biogenic carbon export in the Gulf of St. Lawrence. Continental Shelf Research, 221, 104418, https://doi.org/10.1016/j.csr.2021.104418, 2021.

Gleiber, M.R., Steinberg, D.K. and Ducklow, H.W.: Time series of vertical flux of zooplankton fecal pellets on the continental shelf of the western Antarctic Peninsula. Marine Ecology Progress Series, 471, 23-36, https://doi.org/10.3354/meps10021, 2012.

Golombek, N.Y., Kienast, M., Pilskaln, C.H., Algar, C. and Sherwood, O.: Origin and alteration of sinking and resuspended organic matter on a benthic nepheloid layer influenced continental shelf. Geochimica et Cosmochimica Acta, 366, 31-47, 2024.

Gosselin, M., Levasseur, M., Wheeler, P.A., Horner, R.A. and Booth, B.C.: New measurements of phytoplankton and ice algal production in the Arctic Ocean. Deep Sea Research Part II: Topical Studies in Oceanography, 44(8), 1623-1644, https://doi.org/10.1016/S0967-0645(97)00054-4, 1997.

Grainger, E.H. and Hsiao, S.I.: Trophic relationships of the sea ice meiofauna in Frobisher Bay, Arctic Canada. Polar Biology, 10(4), 283-292, 1990.

Grebmeier, J.M.: Shifting patterns of life in the Pacific Arctic and sub-Arctic seas. Annual Review of Marine Science, 4, 63-78, 2012.

Griffiths, J.R., Kadin, M., Nascimento, F.J., Tamelander, T., Törnroos, A., Bonaglia, S., Bonsdorff, E., Brüchert, V., Gårdmark, A., Järnström, M. and Kotta, J., The importance of benthic–pelagic coupling for marine ecosystem functioning in a changing world. Global Change Biology, 23(6), 2179-2196, https://doi.org/10.1111/gcb.13642, 2017.

Guidi, L., Stemmann, L., Jackson, G.A., Ibanez, F., Claustre, H., Legendre, L., Picheral, M. and Gorskya, G.: Effects of phytoplankton community on production, size, and export of large aggregates: A world-ocean analysis. Limnology and Oceanography, 54(6), 1951-1963, https://doi.org/10.4319/lo.2009.54.6.1951, 2009.

Gutiérrez-Rodríguez, A., Décima, M., Popp, B.N. and Landry, M.R.: Isotopic invisibility of protozoan trophic steps in marine food webs. Limnology and Oceanography, 59(5), 1590-1598, https://doi.org/10.4319/lo.2014.59.5.1590, 2014.

Hall, F.R., Andrews, J.T., Jennings, A., Vilks, G. and Moran, K.: Late Quaternary sediments and chronology of the northeast Labrador Shelf (Karlsefni Trough, Saglek Bank): links to glacial history. Geological Society of America Bulletin, 111(11), 1700-1713, 1999.

Han, G., Ma, Z., Long, Z., Perrie, W. and Chassé, J.: Climate change on Newfoundland and Labrador shelves: Results from a regional downscaled ocean and sea-ice model under an A1B forcing scenario 2011–2069, Atmos. – Ocean, 57(1), 3-17, https://doi.org/10.1080/07055900.2017.1417110, 2019.

Harding, G.C.: 6.4 Submarine Canyons: Deposition Centres for Detrital Organic Matter?. Deep-Sea Res, 2(41), 231-252, 1998.

Hargrave, B.T., Von Bodungen, B., Stoffyn-Egli, P. and Mudie, P.J.: Seasonal variability in particle sedimentation under permanent ice cover in the Arctic Ocean. Continental Shelf Research, 14(2-3), 279-293, 1994.

Harrison, W.G. and Li, W.K.: Phytoplankton growth and regulation in the Labrador Sea: light and nutrient limitation. Journal of Northwest Atlantic Fishery Science, 39, https://doi.org/10.2960/J.v39.m592, 2007.

Harrison, W.G., Børsheim, K.Y., Li, W.K., Maillet, G.L., Pepin, P., Sakshaug, E., Skogen, M.D. and Yeats, P.A.: Phytoplankton production and growth regulation in the Subarctic North Atlantic: A comparative study of the Labrador Sea-Labrador/Newfoundland shelves and Barents/Norwegian/Greenland seas and shelves. Progress in Oceanography, 114, 26-45, https://doi.org/10.1016/j.pocean.2013.05.003, 2013.

Harvey, H.R., O'Hara, S.C., Eglinton, G. and Corner, E.D.: The comparative fate of dinosterol and cholesterol in copepod feeding: implications for a conservative molecular biomarker in the marine water column. Organic Geochemistry, 14(6), 635-641, https://doi.org/10.1016/0146-6380(89)90042-9, 1989.

Hayes, J.M.: Factors controlling 13C contents of sedimentary organic compounds: principles and evidence. Marine Geology, 113(1-2), 111-125, https://doi.org/10.1016/0025-3227(93)90153-M, 1993.

Hecker, B., Blechschmidt, G. and Gibson, P.: Canyon assessment study in the Mid and North Atlantic areas of the US Outer Continental Shelf: epifaunal zonation and community structure in three mid and north Atlantic canyons. Final Report, US Department of the Interior, Bureau of Land Management. Washington, DC, 1980.

Hedges, J.I., Baldock, J.A., Gélinas, Y., Lee, C., Peterson, M. and Wakeham, S.G.: Evidence for non-selective preservation of organic matter in sinking marine particles. Nature, 409(6822), 801-804, https://doi.org/10.1038/35057247, 2001.

Honjo, S. and Doherty, K.W.: Large aperture time-series sediment traps; design objectives, construction and application. Deep Sea Research Part A. Oceanographic Research Papers, 35(1), 133-149, https://doi.org/10.1016/0198-0149(88)90062-3, 1988.

Hsiao, S.I., Quantitative composition, distribution, community structure and standing stock of sea ice microalgae in the Canadian Arctic. Arctic, 768-793, 1980.

Hwang, J., Druffel, E.R. and Eglinton, T.I.: Widespread influence of resuspended sediments on oceanic particulate organic carbon: Insights from radiocarbon and aluminum contents in sinking particles. Global Biogeochemical Cycles, 24(4), https://doi.org/10.1029/2010GB003802, 2010.

Hwang, J., Manganini, S.J., Park, J., Montluçon, D.B., Toole, J.M. and Eglinton, T.I.: Biological and physical controls on the flux and characteristics of sinking particles on the N orthwest A tlantic margin. Journal of Geophysical Research: Oceans, 122(6), 4539-4553, https://doi.org/10.1002/2016JC012549, 2017.

Ianiri, H.L. and McCarthy, M.D.: Compound specific δ15N analysis of amino acids reveals unique sources and differential cycling of high and low molecular weight marine dissolved organic nitrogen. Geochimica et Cosmochimica Acta, https://doi.org/10.1016/j.gca.2023.01.008, 2023.

Irwin, B.D.: Primary production of ice algae on a seasonally-ice-covered, continental shelf. Polar biology, 10(4), pp.247-254, https://doi.org/10.1007/BF00238421, 1990.

Jackson, A.L., Inger, R., Parnell, A.C. and Bearhop, S.: Comparing isotopic niche widths among and within communities: SIBER–Stable Isotope Bayesian Ellipses in R. Journal of Animal Ecology, 80(3), 595-602, 2011.

Juul-Pedersen, T., Michel, C. and Gosselin, M.: Sinking export of particulate organic material from the euphotic zone in the eastern Beaufort Sea. Marine Ecology Progress Series, 410, 55-70, 2010.

Kaiser, K. and Benner, R.: Hydrolysis-induced racemization of amino acids. Limnology and Oceanography: Methods, 3(8), 318-325, https://doi.org/10.4319/lom.2005.3.318, 2005.

Kaltin, S., Anderson, L.G., Olsson, K., Fransson, A. and Chierici, M.: Uptake of atmospheric carbon dioxide in the Barents Sea. Journal of Marine Systems, 38(1-2), 31-45, 2002.

Kaltin, S. and Anderson, L.G.: Uptake of atmospheric carbon dioxide in Arctic shelf seas: evaluation of the relative importance of processes that influence pCO2 in water transported over the Bering–Chukchi Sea shelf. Marine Chemistry, 94(1-4), 67-79, 2005.

Lalande, C., Forest, A., Barber, D.G., Gratton, Y. and Fortier, L.: Variability in the annual cycle of vertical particulate organic carbon export on Arctic shelves: Contrasting the Laptev Sea, Northern Baffin Bay and the Beaufort Sea. Continental Shelf Research, 29(17), 2157-2165, 2009a.

Lalande, C., Bélanger, S. and Fortier, L.: Impact of a decreasing sea ice cover on the vertical export of particulate organic carbon in the northern Laptev Sea, Siberian Arctic Ocean. Geophysical Research Letters, 36(21), 2009b.

Lalande, C., Bauerfeind, E. and Nöthig, E.M.: Downward particulate organic carbon export at high temporal resolution in the eastern Fram Strait: influence of Atlantic Water on flux composition. Marine Ecology Progress Series, 440, 127-136, 2011.

Lalande, C., Nöthig, E.M. and Fortier, L.: Algal export in the Arctic Ocean in times of global warming. Geophysical Research Letters, 46(11), 5959-5967, https://doi.org/10.1029/2019GL083167, 2019.

Larsen, T., Taylor, D.L., Leigh, M.B. and O'Brien, D.M.: Stable isotope fingerprinting: a novel method for identifying plant, fungal, or bacterial origins of amino acids. Ecology, 90(12), 3526-3535, https://doi.org/10.1890/08-1695.1, 2009.

Larsen, T., Ventura, M., Andersen, N., O'Brien, D. M., Piatkowski, U., & McCarthy, M. D.: Tracing carbon sources through aquatic and terrestrial food webs using amino acid stable isotope fingerprinting, PloS One, 8(9). Doi: https://doi.org/10.1371/journal.pone.0073441, 2013.

Larsen, T., Bach, L.T., Salvatteci, R., Wang, Y.V., Andersen, N., Ventura, M. and McCarthy, M.D.: Assessing the potential of amino acid 13 C patterns as a carbon source tracer in marine sediments: effects of algal growth conditions and sedimentary diagenesis. Biogeosciences, 12(16), 4979-4992, https://doi.org/10.5194/bg-12-4979-2015, 2015.

Leblanc, K., Arístegui, J., Armand, L., Assmy, P., Beker, B., Bode, A., Breton, E., Cornet, V., Gibson, J., Gosselin, M.P. and Kopczynska, E.: A global diatom database–abundance, biovolume and biomass in the world ocean. Earth System Science Data, 4(1), 149-165, https://doi.org/10.5194/essd-4-149-2012, 2012.

Lehman, J.: Compound-specific amino acid isotopes as tracers of algal central metabolism: developing new tools for tracing prokaryotic vs. eukaryotic primary production and organic nitrogen in the ocean. University of California, Santa Cruz, CA, Santa Cruz, CA, 2009.

Le Moigne, F.A., Poulton, A.J., Henson, S.A., Daniels, C.J., Fragoso, G.M., Mitchell, E., Richier, S., Russell, B.C., Smith, H.E., Tarling, G.A. and Young, J.R.: Carbon export efficiency and phytoplankton community composition in the A tlantic sector of the A rctic O cean. Journal of Geophysical Research: Oceans, 120(6), 3896-3912, https://doi.org/10.1002/2015JC010700, 2015.

Leu, E., Mundy, C.J., Assmy, P., Campbell, K., Gabrielsen, T.M., Gosselin, M., Juul-Pedersen, T. and Gradinger, R.: Arctic spring awakening–Steering principles behind the phenology of vernal ice algal blooms. Progress in Oceanography, 139, 151-170, https://doi.org/10.1016/j.pocean.2015.07.012, 2015.

Levin, L.A. and Le Bris, N.: The deep ocean under climate change. Science, 350(6262), 766-768, 2015.Li, W.K., McLaughlin, F.A., Lovejoy, C. and Carmack, E.C.: Smallest algae thrive as the Arctic Ocean freshens. Science, 326(5952), 539-539, https://www.science.org/doi/full/10.1126/science.1179798, 2009.

Li, W.K., McLaughlin, F.A., Lovejoy, C. and Carmack, E.C.: Smallest algae thrive as the Arctic Ocean freshens. Science, 326(5952), 539-539, 2009.

Longhurst, A.R.: Ecological geography of the sea. Elsevier, 2010.

Lund, J.W.G., Kipling, C. and Le Cren, E.D.: The inverted microscope method of estimating algal numbers and the statistical basis of estimations by counting. Hydrobiologia, 11, 143-170, https://doi.org/10.1007/BF00007865, 1958.

MacGilchrist, G.A., Garabato, A.N., Tsubouchi, T., Bacon, S., Torres-Valdés, S. and Azetsu-Scott, K.: The arctic ocean carbon sink. Deep Sea Research Part I: Oceanographic Research Papers, 86, 39-55, 2014.

Macko, S.A., Helleur, R., Hartley, G. and Jackman, P.: Diagenesis of organic matter—a study using stable isotopes of individual carbohydrates. Organic Geochemistry, 16(4-6), 1129-1137, 1990.

Marson, J.M., Myers, P.G., Hu, X. and Le Sommer, J.: Using vertically integrated ocean fields to characterize Greenland icebergs' distribution and lifetime. Geophysical Research Letters, 45(9), 4208-4217, 2018.

McCarthy, M.D., Benner, R., Lee, C. and Fogel, M.L.: Amino acid nitrogen isotopic fractionation patterns as indicators of heterotrophy in plankton, particulate, and dissolved organic matter. Geochimica et Cosmochimica Acta, 71(19), 4727-4744, https://doi.org/10.1016/j.gca.2007.06.061, 2007.

McCarthy, M.D., Lehman, J. and Kudela, R.: Compound-specific amino acid δ15N patterns in marine algae: Tracer potential for cyanobacterial vs. eukaryotic organic nitrogen sources in the ocean. Geochimica et cosmochimica Acta, 103, 104-120, https://doi.org/10.1016/j.gca.2012.10.037, 2013.

McClelland, J.W. and Montoya, J.P.: Trophic relationships and the nitrogen isotopic composition of amino acids in plankton. Ecology, 83(8), 2173-2180, https://doi.org/10.1890/0012-9658(2002)083[2173:TRATNI]2.0.CO;2, 2002.

McDonnell, A.M., Lam, P.J., Lamborg, C.H., Buesseler, K.O., Sanders, R., Riley, J.S., Marsay, C., Smith, H.E., Sargent, E.C., Lampitt, R.S. and Bishop, J.K.: The oceanographic toolbox for the collection of sinking and suspended marine particles. Progress in Oceanography, 133, 17-31, 2015.

McMahon, K.W., Ambrose Jr, W.G., Johnson, B.J., Sun, M.Y., Lopez, G.R., Clough, L.M. and Carroll, M.L.: Benthic community response to ice algae and phytoplankton in Ny Ålesund, Svalbard. Marine Ecology Progress Series, 310, 1-14, doi:10.3354/meps310001, 2006.

McMahon, K.W., Hamady, L.L. and Thorrold, S.R.: Ocean ecogeochemistry: a review. Oceanography and Marine Biology, 335-398, 2013.

McMahon, K. W., McCarthy, M. D., Sherwood, O. A., Larsen, T., & Guilderson, T. P.: Millennial-scale plankton regime shifts in the subtropical North Pacific Ocean. Science, 350(6267), 1530-1533, https://www.science.org/doi/10.1126/science.aaa9942, 2015.

McMahon, K.W. and McCarthy, M.D.: Embracing variability in amino acid δ15N fractionation: mechanisms, implications, and applications for trophic ecology. Ecosphere, 7(12), e01511, https://doi.org/10.1002/ecs2.1511, 2016.

McQuatters-Gollop, A., Johns, D.G., Bresnan, E., Skinner, J., Rombouts, I., Stern, R., Aubert, A., Johansen, M., Bedford, J. and Knights, A.: From microscope to management: the critical value of plankton taxonomy to marine policy and biodiversity conservation. Marine Policy, 83, 1-10, https://doi.org/10.1016/j.marpol.2017.05.022, 2017.

Melnikov, I.A.: Winter production of sea ice algae in the western Weddell Sea. Journal of Marine Systems, 17(1-4), 195-205, 1998.

Michaels, A.F. and Silver, M.W.: Primary production, sinking fluxes and the microbial food web. Deep Sea Research Part A. Oceanographic Research Papers, 35(4), 473-490, https://doi.org/10.1016/0198-0149(88)90126-4, 1988.

Michel, C., Legendre, L., Therriault, J.C., Demers, S. and Vandevelde, T.: Springtime coupling between ice algal and phytoplankton assemblages in southeastern Hudson Bay, Canadian Arctic. Polar Biology, 13, 441-449, 1993.

Michel, C., Legendre, L., Ingram, R.G., Gosselin, M. and Levasseur, M.: Carbon budget of sea‐ice algae in spring: Evidence of a significant transfer to zooplankton grazers. Journal of Geophysical Research: Oceans, 101(C8), 18345-18360, 1996.

Michel, C., Nielsen, T.G., Nozais, C. and Gosselin, M.: Significance of sedimentation and grazing by ice micro-and meiofauna for carbon cycling in annual sea ice (northern Baffin Bay). Aquatic Microbial Ecology, 30(1), 57-68, 2002.

Michel, C., Ingram, R.G. and Harris, L.R.: Variability in oceanographic and ecological processes in the Canadian Arctic Archipelago. Progress in Oceanography, 71(2-4), 379-401, 2006.

Montes, E., Thunell, R., Muller-Karger, F.E., Lorenzoni, L., Tappa, E., Troccoli, L., Astor, Y. and Varela, R.: Sources of δ15N variability in sinking particulate nitrogen in the Cariaco Basin, Venezuela. Deep Sea Research Part II: Topical Studies in Oceanography, 93, 96-107, https://doi.org/10.1016/j.dsr2.2013.01.006, 2013.

Mouw, C.B., Barnett, A., McKinley, G.A., Gloege, L. and Pilcher, D.: Phytoplankton size impact on export flux in the global ocean. Global Biogeochemical Cycles, 30(10), 1542-1562, https://doi.org/10.1002/2015GB005355, 2016.

Mundy, C.J., Gosselin, M., Ehn, J., Gratton, Y., Rossnagel, A., Barber, D.G., Martin, J., Tremblay, J.É., Palmer, M., Arrigo, K.R. and Darnis, G.: Contribution of under‐ice primary production to an ice‐edge upwelling phytoplankton bloom in the Canadian Beaufort Sea. Geophysical Research Letters, 36(17), 2009.

Mundy, C.J., Gosselin, M., Gratton, Y., Brown, K., Galindo, V., Campbell, K., Levasseur, M., Barber, D., Papakyriakou, T. and Bélanger, S.: Role of environmental factors on phytoplankton bloom initiation under landfast sea ice in Resolute Passage, Canada. Marine Ecology Progress Series, 497, 39-49, 2014.

Murata, A. and Takizawa, T.: Summertime CO2 sinks in shelf and slope waters of the western Arctic Ocean. Continental Shelf Research, 23(8), 753-776, 2003.

Nakatsuka, T., Handa, N., Harada, N., Sugimoto, T. and Imaizumi, S.: Origin and decomposition of sinking particulate organic matter in the deep water column inferred from the vertical distributions of its δ15N, δ13 and δ14. Deep Sea Research Part I: Oceanographic Research Papers, 44(12), 1957-1979, https://doi.org/10.1016/S0967-0637(97)00051-4, 1997.

Nielsen, J.M., Popp, B.N. and Winder, M.: Meta-analysis of amino acid stable nitrogen isotope ratios for estimating trophic position in marine organisms. Oecologia, 178(3), 631-642, https://doi.org/10.1007/s00442-015-3305-7, 2015.

Noji, T.T.: The influence of icrozooplankton on vertical particulate flux. Sarsia, 76(1-2), 1-9, https://doi.org/10.1080/00364827.1991.10413459, 1991.

North, C.A., Lovvorn, J.R., Kolts, J.M., Brooks, M.L., Cooper, L.W. and Grebmeier, J.M.: Deposit-feeder diets in the Bering Sea: potential effects of climatic loss of sea ice-related microalgal blooms. Ecological Applications, 24(6), 1525-1542, https://doi.org/10.1890/13-0486.1, 2014.

Nowicki, M., DeVries, T. and Siegel, D.A.: Quantifying the carbon export and sequestration pathways of the ocean's biological carbon pump. Global Biogeochemical Cycles, 36(3), e2021GB007083, https://doi.org/10.1029/2021GB007083, 2022.

Ohkouchi, N., Chikaraishi, Y., Close, H.G., Fry, B., Larsen, T., Madigan, D.J., McCarthy, M.D., McMahon, K.W., Nagata, T., Naito, Y.I. and Ogawa, N.O.: Advances in the application of amino acid nitrogen isotopic analysis in ecological and biogeochemical studies. Organic Geochemistry, 113, 150-174, https://doi.org/10.1016/j.orggeochem.2017.07.009, 2017.

Omand, M.M., D'Asaro, E.A., Lee, C.M., Perry, M.J., Briggs, N., Cetinić, I. and Mahadevan, A.: Eddy-driven subduction exports particulate organic carbon from the spring bloom. Science, 348(6231), 222-225, 2015.

Ostiguy, J.: Ambient noise levels off the coast of Northern Labrador (Doctoral dissertation, Memorial University of Newfoundland), 2022.

Pabi, S., van Dijken, G.L. and Arrigo, K.R.: Primary production in the Arctic Ocean, 1998–2006. Journal of Geophysical Research: Oceans, 113(C8), https://doi.org/10.1029/2007JC004578, 2008.

Park, S., Brett, M.T., MÜLLER‐NAVARRA, D.C. and Goldman, C.R.: Essential fatty acid content and the phosphorus to carbon ratio in cultured algae as indicators of food quality for Daphnia. Freshwater Biology, 47(8), 1377-1390, 2002.

Passow, U. and Carlson, C.A.: The biological pump in a high CO2 world. Marine Ecology Progress Series, 470, 249-271, https://doi.org/10.3354/meps09985, 2012.

Peterson, B.J. and Fry, B.: Stable isotopes in ecosystem studies. Annual Review of Ecology and Systematics, 18(1), 293-320, https://doi.org/10.1146/annurev.es.18.110187.001453, 1987.

Pilskaln, C.H. and Honjo, S.: The fecal pellet fraction of biogeochemical particle fluxes to the deep sea. Global Biogeochemical Cycles, 1(1), 31-48, https://doi.org/10.1029/GB001i001p00031, 1987.

Post, E., Bhatt, U.S., Bitz, C.M., Brodie, J.F., Fulton, T.L., Hebblewhite, M., Kerby, J., Kutz, S.J., Stirling, I. and Walker, D.A.: Ecological consequences of sea-ice decline. Science, 341(6145), 519-524, https://www.science.org/doi/10.1126/science.1235225, 2013.

Poulin, M., Daugbjerg, N., Gradinger, R., Ilyash, L., Ratkova, T. and von Quillfeldt, C.: The pan-Arctic biodiversity of marine pelagic and sea-ice unicellular eukaryotes: a first-attempt assessment. Marine Biodiversity, 41(1), 13-28, https://doi.org/10.1007/s12526-010-0058-8, 2011.

Rashid, H., Piper, D.J., Lazar, K.B., McDonald, K. and Saint-Ange, F.: The Holocene Labrador Current: Changing linkages to atmospheric and oceanographic forcing factors, Paleoceanography, 32(5), 498-510, https://doi.org/10.1002/2016PA003051, 2017.

Rau, G.H., Chavez, F.P. and Friederich, G.E.: Plankton 13C/12C variations in Monterey Bay, California: evidence of non-diffusive inorganic carbon uptake by phytoplankton in an upwelling environment. Deep Sea Research Part I: Oceanographic Research Papers, 48(1), 79-94, https://doi.org/10.1016/S0967-0637(00)00039-X, 2001.

Rea, D.K. and Hovan, S.A.: Grain size distribution and depositional processes of the mineral component of abyssal sediments: Lessons from the North Pacific. Paleoceanography, 10(2), 251-258, https://doi.org/10.1029/94PA03355, 1995.

Redfield, A. C., B. H. Ketchum, and F. A. Richards. "The influence of organisms on the composition of seawater." The Sea 2 (1963): 26-77.

Riebesell, U., Körtzinger, A. and Oschlies, A.: Sensitivities of marine carbon fluxes to ocean change. Proceedings of the National Academy of Sciences, 106(49), 20602-20609, https://doi.org/10.1073/pnas.0813291106, 2009.

Rumolo, P., M. Barra, S. Gherardi, E. Marsella, and M. Sprovieri. "Stable isotopes and C/N ratios in marine sediments as a tool for discriminating anthropogenic impact." Journal of Environmental Monitoring 13, no. 12 (2011): 3399-3408.

Runge, J.A. and Ingram, R.G.: Underice grazing by planktonic, calanoid copepods in relation to a bloom of ice microalgae in southeastern Hudson Bay. Limnology and Oceanography, 33(2), 280-286, 1988.

Rysgaard, S., Glud, R.N., Sejr, M.K., Bendtsen, J. and Christensen, P.B.: Inorganic carbon transport during sea ice growth and decay: A carbon pump in polar seas. Journal of Geophysical Research: Oceans, 112(C3), 2007.

Sabadel, A.J.M., Van Oostende, N., Ward, B.B., Woodward, E.M.S., Van Hale, R. and Frew, R.D.: Characterization of particulate organic matter cycling during a summer North Atlantic phytoplankton bloom using amino acid C and N stable isotopes. Marine Chemistry, 214, 103670, https://doi.org/10.1016/j.marchem.2019.103670, 2019.

Sabine, C.L., Feely, R.A., Gruber, N., Key, R.M., Lee, K., Bullister, J.L., Wanninkhof, R., Wong, C.S.L., Wallace, D.W., Tilbrook, B. and Millero, F.J.: The oceanic sink for anthropogenic CO2. Science, 305(5682), 367-371, 2004.

Sabine, C.L. and Tanhua, T.: Estimation of anthropogenic CO2 inventories in the ocean. Annual Review of Marine Science, 2, 175-198, 2010.

Sachs, J.P., Repeta, D.J. and Goericke, R.: Nitrogen and carbon isotopic ratios of chlorophyll from marine phytoplankton. Geochimica et Cosmochimica Acta, 63(9), 1431-1441, 1999.

Sampei, M., Sasaki, H., Hattori, H., Fukuchi, M. and Hargrave, B.T.: Fate of sinking particles, especially fecal pellets, within the epipelagic zone in the North Water (NOW) polynya of northern Baffin Bay. Marine Ecology Progress Series, 278, 17-25, 2004.

Schiff, J.T., Batista, F.C., Sherwood, O.A., Guilderson, T.P., Hill, T.M., Ravelo, A.C., McMahon, K.W. and McCarthy, M.D.: Compound specific amino acid δ13C patterns in a deep-sea proteinaceous coral: Implications for reconstructing detailed δ13C records of exported primary production. Marine Chemistry, 166, 82-91, https://doi.org/10.1016/j.marchem.2014.09.008, 2014.

Schlitzer, R., Ocean Data View, odv.awi.de, 2021.

Schnetzer, A. and Steinberg, D.: Natural diets of vertically migrating zooplankton in the Sargasso Sea. Marine Biology, 141, 89-99, https://doi.org/10.1007/s00227-002-0815-8, 2002.

Schubert, C.J. and Calvert, S.E., Nitrogen and carbon isotopic composition of marine and terrestrial organic matter in Arctic Ocean sediments:: implications for nutrient utilization and organic matter composition. Deep Sea Research Part I: Oceanographic Research Papers, 48(3), 789-810, https://doi.org/10.1016/S0967-0637(00)00069-8, 2001.

Scott, C.L., Falk-Petersen, S., Sargent, J.R., Hop, H., Lønne, O.J. and Poltermann, M.: Lipids and trophic interactions of ice fauna and pelagic zooplankton in the marginal ice zone of the Barents Sea. Polar Biology, 21, 65-70, 1999.

Scott, C.L., Falk-Petersen, S., Gulliksen, B., Lønne, O.J. and Sargent, J.R.: Lipid indicators of the diet of the sympagic amphipod Gammarus wilkitzkii in the Marginal Ice Zone and in open waters of Svalbard (Arctic). Polar Biology, 24, 572-576, 2001.

Shen, Y., Guilderson, T.P., Sherwood, O.A., Castro, C.G., Chavez, F.P. and McCarthy, M.D.: Amino acid δ13C and δ15N patterns from sediment trap time series and deep-sea corals: Implications for biogeochemical and ecological reconstructions in paleoarchives. Geochimica et Cosmochimica Acta, 297, 288-307, https://doi.org/10.1016/j.gca.2020.12.012, 2021.

Sherwood, O.A., Heikoop, J.M., Scott, D.B., Risk, M.J., Guilderson, T.P. and McKinney, R.A.: Stable isotopic composition of deep-sea gorgonian corals Primnoa spp.: a new archive of surface processes. Marine Ecology Progress Series, 301, 135-148, doi:10.3354/meps301135, 2005.

Sherwood, O.A. and Edinger, E.N.: Ages and growth rates of some deep-sea gorgonian and antipatharian corals of Newfoundland and Labrador. Canadian Journal of Fisheries and Aquatic Sciences, 66(1), 142-152, https://doi.org/10.1139/F08-195, 2009.

Sherwood, O.A., Lehmann, M.F., Schubert, C.J., Scott, D.B. and McCarthy, M.D.: Nutrient regime shift in the western North Atlantic indicated by compound-specific δ 15N of deep-sea gorgonian corals. Proceedings of the National Academy of Sciences, 108(3), 1011-1015, https://doi.org/10.1073/pnas.1004904108, 2011.

Sherwood, O.A., Davin, S.H., Lehmann, N., Buchwald, C., Edinger, E.N., Lehmann, M.F. and Kienast, M.: Stable isotope ratios in seawater nitrate reflect the influence of Pacific water along the northwest Atlantic margin. Biogeosciences, 18(15), pp.4491-4510, 2021.

Silfer, J. A., Engel, M. H., Macko, S. A., & Jumeau, E. J.: Stable carbon isotope analysis of amino acid enantiomers by conventional isotope ratio mass spectrometry and combined gas chromatography/isotope ratio mass spectrometry, Analytical Chemistry, 63(4), 370-374, https://doi.org/10.1021/ac00004a014, 1991.

Søreide, J.E., Hop, H., Carroll, M.L., Falk-Petersen, S. and Hegseth, E.N.: Seasonal food web structures and sympagic–pelagic coupling in the European Arctic revealed by stable isotopes and a two-source food web model. Progress in Oceanography, 71(1), 59-87, https://doi.org/10.1016/j.pocean.2006.06.001, 2006.

Stahl, A.: Identifying Novel Isotopic Tracers of Marine Primary Producers to Study Food Web Carbon Cycles (Doctoral dissertation, University of Rhode Island), 2021.

Stamieszkin, K., Steinberg, D.K. and Maas, A.E.: Fecal pellet production by mesozooplankton in the subarctic Northeast Pacific Ocean. Limnology and Oceanography, 66(7), 2585-2597, https://doi.org/10.1002/lno.11774, 2021.

Steele, M., Ermold, W. and Zhang, J.: Arctic Ocean surface warming trends over the past 100 years. Geophysical Research Letters, 35(2), 2008.

Stock, B. and Semmens, B.: MixSIAR GUI user manual v3. 1. Scripps Institution of Oceanography, UC San Diego, San Diego, California, USA, 2016.

Strass, V.H. and Nöthig, E.M.: Seasonal shifts in ice edge phytoplankton blooms in the Barents Sea related to the water column stability. Polar Biology, 16, 409-422, 1996.

Sweetman, A.K., Thurber, A.R., Smith, C.R., Levin, L.A., Mora, C., Wei, C.L., Gooday, A.J., Jones, D.O., Rex, M., Yasuhara, M. and Ingels, J.: Major impacts of climate change on deep-sea benthic ecosystems. Elementa: Science of the Anthropocene, 5, 4, 2017.

Turner, J.T.: Zooplankton fecal pellets, marine snow, phytodetritus and the ocean's biological pump. Progress in Oceanography, 130, 205-248, https://doi.org/10.1016/j.pocean.2014.08.005, 2015.

Vokhshoori, N.L., Larsen, T. and McCarthy, M.D.: Reconstructing δ13C isoscapes of phytoplankton production in a coastal upwelling system with amino acid isotope values of littoral mussels. Marine Ecology Progress Series, 504, 59-72, https://doi.org/10.3354/meps10746, 2014.

Volk, T. and Hoffert, M.I.: Ocean carbon pumps: Analysis of relative strengths and efficiencies in ocean ‐ driven atmospheric CO2 changes. The carbon cycle and atmospheric CO2: Natural variations Archean to present, 32, 99-110, 1985.

Wakeham, S.G. and Canuel, E.A.: Organic geochemistry of particulate matter in the eastern tropical North Pacific Ocean: Implications for particle dynamics. Journal of Marine Research, 46(1), 183-213, https://doi.org/10.1357/002224088785113748, 1988.

Wareham, V.E. and Edinger, E.N.: Distribution of deep-sea corals in the Newfoundland and Labrador region, Northwest Atlantic Ocean, Bulletin of Marine Science, 81(3), 289-313, 2007.

Wilson, S.E., Ruhl, H.A. and Smith, Jr, K.L.: Zooplankton fecal pellet flux in the abyssal northeast Pacific: A 15 year time-series study. Limnology and Oceanography, 58(3), 881-892, https://doi.org/10.4319/lo.2013.58.3.0881, 2013.

Wojtal, P.K., Doherty, S.C., Shea, C.H., Popp, B.N., Benitez ‐ Nelson, C.R., Buesseler, K.O., Estapa, M.L., Roca ‐ Martí, M. and Close, H.G.: Deconvolving mechanisms of particle flux attenuation using nitrogen isotope analyses of amino acids. Limnology and Oceanography, 68(9), 1965-1981, 2023.

Yager, P.L., Connelly, T.L., Mortazavi, B., Wommack, K.E., Bano, N., Bauer, J.E., Opsahl, S. and Hollibaugh, J.T.: Dynamic bacterial and viral response to an algal bloom at subzero temperatures. Limnology and Oceanography, 46(4), 790-801, 2001.

Yamaguchi, Y.T. and McCarthy, M.D.: Sources and transformation of dissolved and particulate organic nitrogen in the North Pacific Subtropical Gyre indicated by compound-specific δ15N analysis of amino acids. Geochimica et Cosmochimica Acta, 220, 329-347, https://doi.org/10.1016/j.gca.2017.07.036, 2018.

Yarnes, C.T. and Herszage, J.: The relative influence of derivatization and normalization procedures on the compound-specific stable isotope analysis of nitrogen in amino acid, Rapid Communications in Mass Spectrometry, 31(8), 693-704, https://doi.org/10.1002/rcm.7832, 2017.

Yashayaev, I.: Hydrographic changes in the Labrador Sea, 1960–2005. Progress in Oceanography, 73(3-4), 242-276, 2007.